

*« Human subtlety will never devise an invention more beautiful, more simple, or more direct than does Nature because in her inventions, nothing is lacking and nothing is superfluous... »*

**Leonardo da Vinci**

# Acknowledgments

And because nothing is done unless we work as a team, I want to thank and show my gratitude to all those who made this possible, and have accompanied me during this last year.

To my supervisor, Professor João Laranjinha, Ph.D., from the Laboratory of Biochemistry at the Faculty of Pharmacy and leader of the group of Redox Biology in Health and Disease (RebHdis) of the Center for Neurosciences and Cell Biology of Coimbra where the work was done, a real friend over the year, for what I learned and for firing me with enthusiasm for the fascinating world that is science!!!

To Cátia Marques, from group RebHdis at Center for Neurosciences and Cell Biology, for contributing decisively to the work, providing guidance whenever she was present that having taught me so much, thank you very much.

To Professor Rui Barbosa, Ph.D., and other laboratory colleagues of RebHdis, always present in any situation, day-to-day, for sharing experiences, knowledge, jokes and fun, essential for good performance in the laboratory.

To all my friends who helped me in many ways, during the accomplishment of this work, through their support in each moment! Thank you all!

To my family, and essentially my parents, for the unconditional support and for the greatness that characterizes them, for their patience and understanding throughout my absence. Thanks for the constant encouragement and for having always believed in me!

This work was supported by the projects PTDC/SAU-NEU/108992/2008, PTDC/SAU-NEU/103538/2008 and PTDC/SAU-BEB/103228/2008 funded by Fundação para a Ciência e Tecnologia.

# Index

<b>Acknowledgments</b> .....	<b>II</b>
<b>Index</b> .....	<b>III</b>
<b>Picture Index</b> .....	<b>V</b>
<b>Table Index</b> .....	<b>VII</b>
<b>Abbreviations and Symbols</b> .....	<b>IX</b>
<b>Resumo</b> .....	<b>XII</b>
<b>Abstract</b> .....	<b>XIII</b>
<b>Chapter 1</b> .....	<b>8</b>
<b>Introduction</b> .....	<b>8</b>
<b>I. Nitric oxide</b> .....	<b>9</b>
1. Biochemical Properties and Diffusion of $\cdot\text{NO}$ .....	9
2. The nitric oxide synthase (NOS) .....	11
2.1. Reductase and Oxygenase Domains.....	12
2.2. NO Biosynthesis.....	13
2.3. Regulation of nNOS .....	13
3. Signaling pathways in central nervous system mediated by $\cdot\text{NO}$ .....	14
4. Bioimaging of nitric oxide .....	15
4.1. Electrodes for $\cdot\text{NO}$ detection .....	17
<b>II. Neurovascular coupling</b> .....	<b>18</b>
1. Mechanism of neurovascular coupling .....	19
<b>III. Alzheimer's disease</b> .....	<b>21</b>
1. Bacteria are powerful stimulators of inflammation and are amyloidogenic .....	22
2. Inflammation, $\cdot\text{NO}$ and polyphenolic pathways.....	23
<b>IV. Hypothesis</b> .....	<b>25</b>
<b>Chapter 2</b> .....	<b>27</b>

<b>Materials and Methods .....</b>	<b>27</b>
<b>I. Experimental Design .....</b>	<b>28</b>
<b>II. Chemicals and Solutions.....</b>	<b>29</b>
<b>III. <i>In vivo</i> testing.....</b>	<b>29</b>
1. NO Microelectrodes.....	29
2. Calibration and Selectivity .....	30
2.1. Neurodegenerative rat models .....	32
3. Behavior Tests.....	33
3.1. Open field .....	33
3.2. Novel-Object recognition test .....	33
3.3. Y-maze .....	34
4. Array production.....	34
5. Animals and surgical preparation .....	34
6. Stimulation and pharmacological modulation of $\text{NO}$ with Curcumin and Epicatechin 35	
7. Data analysis .....	35
<b>Chapter 3 .....</b>	<b>37</b>
<b>Results .....</b>	<b>37</b>
<b>I. <i>In vivo</i> Nitric Oxide and cerebral blood flow coupling dynamics .....</b>	<b>38</b>
<b>II. Modulation of neuronal-derived <math>\text{NO}</math> and neurovascular coupling with Polyphenols     39</b>	
1. Curcumin.....	39
2. Epicatechin.....	42
3. Discussion .....	44
<b>III. Dementia and inflammatory animal models .....</b>	<b>46</b>
1. Acute model of Alzheimer Disease .....	46
1.1. Behaviour tests.....	46
1.2. CBF and $\text{NO}$ Dynamics .....	47
1.3. Modulation of neurovascular coupling in AD by Curcumin.....	48
2. Discussion .....	50

3. Lipopolysaccharide (LPS) inflammation induction .....	53
4. Discussion .....	55
<b>Chapter 4.....</b>	<b>57</b>
<b>General Conclusions .....</b>	<b>57</b>
<b>Chapter 6.....</b>	<b>59</b>
<b>References .....</b>	<b>59</b>

## Picture Index

Figure 1- Reactions mediated by $\cdot\text{NO}$ in biological systems. Adapted from (Wink and Mitchell, 1998, Davis <i>et al.</i> , 2001).....	11
Figure 2- NOS structure indicating the oxygenase and reductase domain with binding sites for different cofactors, connected by a calmodulin (CaM) binding site. Adapted from (Lourenço, 2011). .....	12
Figure 3- Glutamatergic synapse. Functional coupling between glutamate NMDA receptor with NOS, and signaling pathways mediated by nitric oxide. Adapted from (Frade, 2007). .....	15
Figure 4- Techniques available for measurement of $\cdot\text{NO}$ (Lourenço, 2011).....	16
Figure 5- Neurovascular coupling mediated by isotropic diffusion NO. Adapted from (Drake and Iadecola, 2007).....	20
Figure 6- The interaction of polyphenols with cellular signaling pathways involved in chronic disease. Flavonoid-induced activation and/or inhibition of MAP kinase and PI3 kinase signaling leads to the activation of transcription factors which drive gene expression (Vazour <i>et al.</i> , 2010). .....	24
Figure 7- Measurement of CBF and $\cdot\text{NO}$ on rat hippocampus. Array consists of laser doppler probe for measure cerebral blood flow (CBF), Stimulus micropipette for glutamate injection, and microelectrode to measure $\cdot\text{NO}$ production. ....	28
Figure 8- Microelectrodes fabrication (A-B) Pulling of the glass capillary with a carbon fiber inside in a vertical puller. (C) Cutting $200 \pm 50 \mu\text{m}$ of fiber under the microscope (Lourenço, 2011). ..	29
Figure 9- Schematic representation of exclusion layers of Nafion® and o-phenylenediamine at the carbon fiber surface. ( <a href="http://www.cnb.pt/research/areaC1_2.asp?lg=2">http://www.cnb.pt/research/areaC1_2.asp?lg=2</a> ). .....	30

Figure 10- Determination of microelectrodes sensitivity for  $\dot{\text{NO}}$  and selectivity against interferences.  
 (A) Representative recording of microelectrode calibration. Compounds were added at the times indicated by the upper arrows. (B) Linear regression applied to the correlation between the concentration of  $\dot{\text{NO}}$  added and the current change resulting from each addition. .... 31

Figure 11- (A) AD induction by intracerebroventricular injection of  $A\beta_{1-42}$ . (B-C) Anesthetic recuperation after surgery, and in detail rat's scalp sutured..... 32

Figure 12- Schematic diagram of a  $\dot{\text{NO}}$  signal to illustrate how signal parameters were measured and calculated, namely the  $[\dot{\text{NO}}]$  *peak*, *area* (shaded),  $T_{\text{rise}}$ ,  $T_{50}$  and  $T_{\text{total}}$ . .... 36

Figure 13- Experimental Schedule..... 36

Figure 14- Representative recording of the simultaneous measurements of  $\dot{\text{NO}}$  produced by local application of L-glutamate on rat hippocampus (bottom, black line) and CBF changes (top, light grey line). L-Glutamate (20 mM, 25 nL) was locally applied at times indicated by the arrows. .... 38

Figure 15- Effect of curcumin in glutamate-induced  $\dot{\text{NO}}$  dynamics (black line) and CBF changes (grey line) in rat hippocampus. L-Glutamate (20 mM, 25 nL) was locally applied at times indicated by the upward arrows. Curcumin was intracerebroventricularly administered (20 mM) at the time indicated by the downward arrow. .... 40

Figure 16- Quantitative analysis of peak  $\dot{\text{NO}}$  concentrations (A) and CBF amplitude (B) before and after curcumin intracerebroventricular injection. Data represents mean  $\pm$  SEM. Statistical analysis was performed by Student's t-test in relation to control experiments..... 40

Figure 17- Quantitative analysis of peak  $\dot{\text{NO}}$  concentrations (A) and CBF amplitude (B) before and after curcumin intraperitoneal injection. Data represents mean  $\pm$  SEM. Statistical analysis was performed by Student's t-test in relation to control experiments. .... 41

Figure 18- Effect of epicatechin in glutamate-induced  $\dot{\text{NO}}$  dynamics (black line) and CBF changes (grey line) in rat hippocampus. L-Glutamate (20 mM, 25 nL) was locally applied at times indicated by the upward arrows. Epicatechin (100  $\mu\text{M}$ ) was injected intracerebroventricularly at the time indicated by the downward arrow..... 42

Figure 19- Quantitative analysis of peak  $\dot{\text{NO}}$  concentrations (A) and CBF amplitude (B) before and after Epicatechin (100  $\mu\text{M}$ ) intracerebroventricular injection. Data represents mean  $\pm$  SEM. Statistical analysis was performed by Student's t-test in relation to control experiments. .... 43

Figure 20- Behavior performance of  $A\beta_{1-42}$ -treated and control rats 15 days after the injection. (A) and (B) represent the spontaneous locomotion evaluated in an open field arena regarding,

respectively, the horizontal and vertical exploration. (C) Performance in novel object recognition test regarding the time spent in exploring a novel object, placed in the arena after a previous trial (2 h before) of exploration of two identical objects. (D) Performance in Y-maze regarding the time spent in exploring a novel arm, blocked in a previous exploration of the maze 2-h before. Data represents mean±SEM (n=5)..... 47

Figure 21- Quantitative comparison of the effect of A $\beta$ <sub>1-42</sub> over glutamate-induced `NO dynamics (A) and CBF changes (B) in rat hippocampus. Data represents mean ± SEM. Statistical analysis was performed by Student’s t-test in relation to control experiments (\**p* < 0.05). ..... 48

Figure 22- Effect of *in vivo* peripheral administration of curcumin (300 mg/kg, IP) in A $\beta$ <sub>1-42</sub>-treated rats in glutamate-induced `NO dynamics (black line) and CBF changes (grey line) in rat hippocampus..... 49

Figure 23- Intracerebroventricular perfusion of brain with 20 µg of LPS followed by oxidation current records (black line), and cerebral blood changes (grey line) after Glu stimulations during approximately 6 hours of inflammation induction. .... 54

Figure 24- Quantitative analysis of the effect of inflammation induced by LPS injected ICV (after 4.5h) and intraperitoneally (after 24 h) over glutamate-induced `NO dynamics (A) and CBF changes (B) in rat hippocampus. Data represents mean ± SEM. .... 54

## Table Index

Table 1- Calibration parameters and selectivity ratios of carbon fiber microelectrodes coated with Nafion and o-PD. (Data are given as mean±SEM). ..... 31

Table 2- Analysis of glutamate-induced `NO signals and CBF changes in hippocampus before and after curcumin injected in intracerebroventricularly..... 41

Table 3- Analysis of glutamate-induced `NO signals and CBF changes in hippocampus before and after curcumin intraperitoneal injection..... 42

Table 4-. Analysis of glutamate-induced `NO signals and CBF changes in hippocampus before and after Epicatechin (100µM) locally applied in hippocampus..... 43

Table 5- Analysis of glutamate-induced  $\cdot$ NO signals and CBF changes in hippocampus of rats injected with  $A\beta_{1-42}$  peptide and controls..... 48

Table 6- Analysis of glutamate-induced  $\cdot$ NO signals and CBF changes in hippocampus of  $A\beta_{1-42}$ -treated rats before and after intraperitoneal injection of curcumin ..... 50

Table 7- Analysis of glutamate-induced  $\cdot$ NO signals and CBF changes in hippocampus before and 4.5 and 24h after LPS-induced inflammation..... 55



## Abbreviations and Symbols

AA	Arachidonic Acid
AD	Alzheimer's disease
Ag/AgCl	Silver/Silver Chloride reference electrode
AMPA	$\alpha$ -amino-3-hydroxy-5-methyl-4- isoxazolepropionic acid
AMPA	$\alpha$ -amino-3-hydroxy-5-methyl-4- isoxazolepropionic acid receptors
AP	Anterior-Posterior
APP	Amyloid Precursor Protein
A $\beta$	$\beta$ -amyloid plaques
A $\beta$ <sub>1-42</sub>	A $\beta$ -amyloid (fragment 1-42)
BACE-1	Beta-secretase 1
BBB	blood brain barrier
CaM	Calmodulin
CBF	Cerebral blood flow
CD14	Cluster of Differentiation 14
cGMP	Cyclic Guanosine Monophosphate
CNS	Central Nervous System
CoA	Coenzyme A
COX	cyclooxygenase
Ctr	Control
Cur	Curcumin
CVD	Cardiovascular Disease
DAF-2	4,5-diaminofluorescein
DAF-2T	Triazolofluorescein
DMSO	Dimethyl sulfoxide
DV	Dorsoventral
EDRF	Endothelium-Derived Relaxing Factor
eNOS	Endothelial isoform of nitric oxide synthase
EPR	Electron Paramagnetic Resonance
ERK	Extracellular-Regulated Kinase

FAD	Flavin Adenine Dinucleotide
FMN	Flavin Mononucleotide
fMRI	Functional Magnetic Resonance Imaging
GABA	$\gamma$ -AminoButyric Acid
GJ	Gap Junctions
GSH	Glutathione
GTP	Guanosine Triphosphate
H <sub>4</sub> B	(6R)-5,6,7,8-tetrahydrobiopterin
HbO <sub>2</sub>	Oxyhemoglobin
ICV	Intracerebroventricular
iNOS	Inducible isoform of Nitric Oxide Synthase
IP	Intraperitoneal
JNK	c-Jun N-terminal kinase
KA	Kainate
K <sub>ATP</sub>	ATP-sensitive potassium channels
L-arg	L-arginine
LDF probe	Laser Doppler Flow probe
LO <sup>·</sup>	Alkoxy radical
LOD	Limit Of Detection
LOO <sup>·</sup>	Peroxy radical
LPS	Lipopolysaccharide
LTD	Long-Term Depression
LTP	Long-Term Potentiation
MAP kinase	Mitogen-Activated Protein kinase
MCAO	Middle Cerebral Artery Occlusion
MDA	Malondialdehyde
ML	Medial-Lateral
mtNOS	Mitochondrial isoform of Nitric Oxide Synthase
Na <sup>+</sup> /K <sup>+</sup> /ATPase	Sodium-Potassium Adenosine Triphosphatase pump
NADPH	Nicotinamide Adenine Dinucleotide Phosphate
NFTs	Neurofibrillary tangles
NF- $\kappa$ B	Nuclear Factor-Kappa B

NMDA	<i>N</i> -Methyl- <i>D</i> -Aspartic Acid
NMDAR	<i>N</i> -Methyl- <i>D</i> -Aspartic Acid Receptor
nNOS	Neuronal isoform of Nitric Oxide Synthase
NOS	Nitric Oxide Synthase
o-PD	o-phenylenediamine
p38	p38 mitogen-activated protein kinases
PA	Parkinson's disease
PAF	Platelet Activating Factor
PBS	Phosphate Buffered Saline
PDI	Protein Disulfide Isomerase
PGE2	Prostaglandin E2
PI	Phosphatidylinositol
PI3 kinase	Phosphatidylinositol 3-kinase
PKC	Protein kinase C
PLA2	Phospholipase A2
PSD-95	Postsynaptic Density Protein 95
RNOS	Reactive oxygen/nitrogen species
RNS	Reactive Nitrogen Species
ROS	Reactive oxygen species
sGC	Soluble guanylate cyclase
SOD	Superoxide Dismutase
TLR-4	Toll-Like Receptor 4
TNF $\alpha$	Tumour Necrosis Factor- $\alpha$

## Resumo

O cérebro, mais do que qualquer outro órgão, é criticamente dependente de um fornecimento contínuo de sangue. Em resultado da actividade neuronal elevada, necessita de oxigénio e glicose rapidamente e em grande quantidade de um modo espacialmente relacionado com picos de actividade metabólica dos neurónios. Assim, para além da regulação extrínseca do fluxo através do “output” cardíaco, o fluxo sanguíneo necessário para o cérebro é assegurado por um acoplamento espacial e temporal entre a actividade neuronal e a microcirculação cerebral correlacionada, que através de mecanismos específicos, permitem um aumento do fluxo sanguíneo numa determinada região, permitindo deste modo, o suprimento de nutrientes energéticos, bem como a eliminação de resíduos decorrentes da actividade neuronal. Esta fina associação permite deste modo, regular o fluxo sanguíneo cerebral (CBF) local. O paradigma actual para este acoplamento envolve uma ponte astrocítica entre neurónios e vasos. Neste trabalho explora-se uma via alternativa que envolve a difusão isotrópica do óxido nítrico dos neurónios até aos vasos sanguíneos, induzindo aumento localizado de fluxo em função da actividade neuronal.

Por outro lado, é sabido que alterações vasculares, ao interromper estes mecanismos vasoregulatórios que asseguram um fornecimento adequado de CBF, causam disfunção cerebral, levando a diferentes patologias, nomeadamente em doenças neurodegenerativas como a doença de Alzheimer.

Assim, através de medição directa das dinâmicas de concentração de óxido nítrico in vivo, em tempo real e, mais ainda, em simulatâneo com alterações de CBF no cérebro de animais normais e de animais manifestando condições neuropatológicas (através da administração de  $A\beta_{1-42}$  assim como de Lipopolissacarídeo), este trabalho fornece novas perspectivas sobre o acoplamento neurovascular, associado ao envelhecimento e neurodegeneração, onde polifenóis provenientes da dieta como a curcumina e a epicatequina, evidenciaram um potencial modulador neste processo de acoplamento.

**Palavras-chave:** Óxido nítrico, Acoplamento Neurovascular, Polifenóis, Doença de Alzheimer, Neuroinflamação.

# Abstract

The brain, more than any other organ, is critically dependent on a continuous supply of blood. Due to the high neuronal activity, it needs oxygen and glucose, faster or in greater quantities and in a way that the energy demands imposed by neuronal activity are spatially and temporally correlated with substrate delivery by blood flow.

Thus, in addition to the regulation of blood flow by extrinsic factors (cardiac output) the brain has the ability to regulate the blood flow intrinsically. This is ensured by a tight connection between the neuronal activity and cerebral microcirculation, which through specific mechanisms, allow an increase of blood flow in a region (functional hyperemia), thereby enabling the supply of nutrients energy and the disposal of waste arising from neuronal activity.

This neurovascular coupling induces a chain of complex biological mechanisms, resulting in a joint action between neurons, glia and blood vessels, called the neurovascular unit. This fine combination allowing the regulation of cerebral blood flow (CBF) has been mechanistically assigned to than astrocytic bridge between neurons and blood vessels. Here, we explore an alternative hypothesis encompassing the isotropic diffusion of nitric oxide from neurons towards blood vessels, thus inducing vasodilation.

It is known that vascular impairment interrupt these vasoregulatory mechanisms, which ensure the adequate supply of CBF, causing brain dysfunction and leading to different diseases including the neurodegenerative, such as Alzheimer'. This work aims to clarify the role of nitric oxide as a neuromodulator in the control of neuronal blood flow, as well as explain the influence of dietary polyphenol compounds (curcumin and epicatechin) in the bioavailability of neuronal nitric oxide.

Thus, by means of in vivo and real-time measuring 'NO concentration dynamics in rat brain in simultaneous with measurement of CBF changes in normal animals and animal models of Alzheimer, expressing neuropathological signs (by administration of A $\beta$ <sub>1-42</sub> as well as Lipopolysaccharide), this study provides new insights into the neurovascular coupling associated with aging and neurodegeneration, where dietary polyphenols such as curcumin and epicatechin, are evidenced as potential modulator in this coupling process.

**Keywords:** Nitric Oxide, Neurovascular coupling, Polyphenols, Alzheimer's Disease, Neuroinflammation.

**Chapter 1.**

# **Introduction**



# I. Nitric oxide

Nitric oxide ( $\text{NO}$ ), a small radical molecule, was identified in biological systems as an important intercellular gas messenger present in the cardiovascular, immune and nervous systems (Koshland, 1992).

During the last three decades, several studies have impart an extraordinary interest to this fascinating molecule, mainly due to its distinct physicochemical properties and diverse bioactivity (Koshland, 1992; Ledo, 2007). In brain,  $\text{NO}$  plays a dual action, being involved in different physiological and pathological processes. It is implicated in the modulation of neuronal function through signaling pathways involved in synaptic plasticity (Prast and Philippu, 2001) and in the regulation of blood flow (MacMicking *et al.*, 1997). However,  $\text{NO}$  also acts in different pathways of cell toxicity associated with neurodegenerative diseases and inflammation (Reis, 2006; Pacher *et al.*, 2007).

## 1. Biochemical Properties and Diffusion of $\text{NO}$

$\text{NO}$  is a molecule with only two atoms, being an intermediate between  $\text{O}_2$  and  $\text{N}_2$ . Contrary to what is conventionally found in the literature,  $\text{NO}$  per se is not very reactive when compared with other O or N-centered radicals (Bonner and Sledman, 1996). In addition to its small size,  $\text{NO}$  is hydrophobic, highly diffusible and has a short half-life (*c.a.* 4 s). The high diffusion coefficient ( $3300 \mu\text{m}^2/\text{s}$ ) and hydrophobicity allows  $\text{NO}$  to readily permeate biological membranes and diffuse to considerably high distances to adjacent cells and organelles (Lancaster, 1994; Koppenol, 1998), from its production site, integrating the activity of several cells in a volume of tissue regardless of whether the cells are connected by synapses (Stryer, 1995). Studies have shown that  $\text{NO}$  can spread to a distance of several microns from its site of synthesis (Miranda *et al.*, 2000). In hippocampal slices, in CA1 subregion, it was demonstrated that  $\text{NO}$  have the ability to spread approximately  $400 \mu\text{m}$  (Ledo, 2007).

Unlike other neurotransmitters,  $\text{NO}$  is not stored in vesicles and do not transmit information specifically on basis of its structural characteristics, but instead by changes in its local concentration, mediating a number of physiological pathways quite differently from other neurotransmitters.

Diffusing isotropically in the CNS, the spatio-temporal profile of  $\cdot\text{NO}$  concentration is determined by regulation of its synthesis and distribution of its molecular targets (Espey *et al.*, 2002). Also, mechanisms of  $\cdot\text{NO}$  degradation are of particular relevance, as physiological processes mediated by  $\cdot\text{NO}$  only finish when its removal is complete (Pacher *et al.*, 2007).

The unique chemistry of  $\cdot\text{NO}$  allows it to participate in numerous reactions and to be involved in a diverse number of biological mechanisms. The chemical biology of  $\cdot\text{NO}$  and its potential reactions can be categorized into two types: direct and indirect (Figure 1).

### *Direct effects*

The direct effects rely on the direct reaction of  $\cdot\text{NO}$  with molecular targets (metal complexes or radical species) and are usually associated with short exposures and/or low  $\cdot\text{NO}$  concentration (Espey *et al.*, 2002).

There are three types of reactions of  $\cdot\text{NO}$  with metals, which highlights the reaction between  $\cdot\text{NO}$  and heme iron, present in some proteins including soluble guanylate cyclase (sGC), the nitric oxide synthase (NOS) and several P450 enzymes (Espey *et al.*, 2002). Another example is the reaction of  $\cdot\text{NO}$  with oxyhemoglobin, forming methemoglobin, which constitutes the main removal pathway from  $\cdot\text{NO}$  in biological systems (Lancaster, 1994, Espey *et al.*, 2002, Santos, 2011).

$\cdot\text{NO}$  also directly reacts with other radical species, particularly with lipid and carbon-centered radicals (alkoxyl -  $\text{LO}\cdot$ , peroxy -  $\text{LOO}\cdot$  etc.), formed as a result of both oxidative stress and normal metabolism. This reaction leads to the terminating of lipid peroxidation chain reactions, and thus affords protection against peroxide-induced cytotoxicity (Padmaja and Huie, 1993)

### *Indirect effects*

Indirect effects are mediated by products of reaction of  $\cdot\text{NO}$  with  $\text{O}_2$  or superoxide radical ( $\text{O}_2^{\cdot-}$ ) to form reactive species of nitrogen/oxygen (RNOS), being related with prolonged and/or high  $\cdot\text{NO}$  concentrations and mainly associated to pathological processes.

In aerobic conditions,  $\cdot\text{NO}$  reacts with  $\text{O}_2$ , leading to the formation of several RNOS, such as nitrogen dioxide radical ( $\cdot\text{NO}_2$ ) and nitrogen trioxide ( $\text{N}_2\text{O}_3$ ) (Bruckdorfer, 2005). Both can nitrosate and oxidize different molecules and are primarily responsible for mediating nitrosative stress *in vivo*



(Schwartz *et al.*, 1983). However, nitrosation is an important signal transduction pathway, being described as a new mechanism of signal transduction regulated by enzymes, similar to phosphorylation (Mannick *et al.*, 2002). S-nitrosation of regulatory proteins influences their functions, which impact in cellular physiology (Jaffrey *et al.*, 2001).

$\cdot\text{NO}$ , is also able to react rapidly with  $\text{O}_2^{\cdot-}$ , producing peroxynitrite ( $\text{ONOO}^-$ ).  $\text{ONOO}^-$ , a very reactive molecule, can directly oxidize protein lipids and nucleic acids and nitrate proteins and lipids, with relevant consequences in several signaling pathways (Radi *et al.*, 1991). It is the main responsible for the cytotoxicity attributed to  $\cdot\text{NO}$ , being involved in neurodegeneration, acute and chronic inflammatory processes, sepsis, ischemia-reperfusion injury and vascular disease (Pacher *et al.*, 2007).

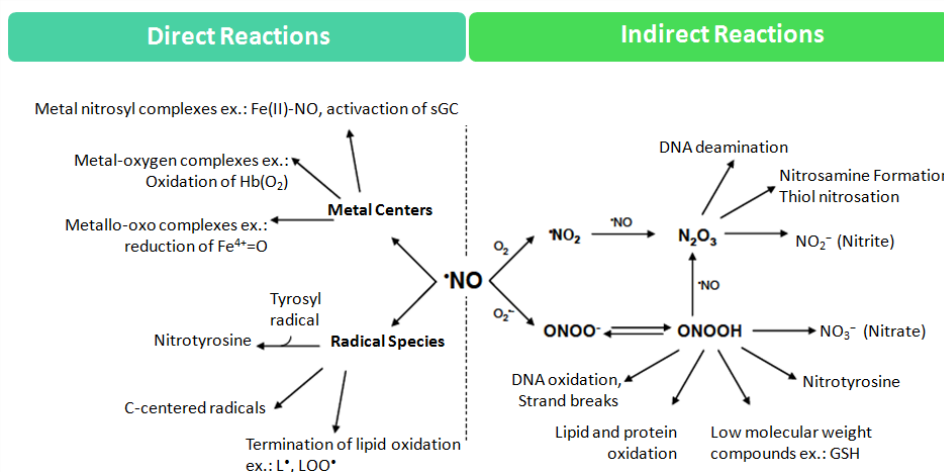


**Figure 1-** Reactions mediated by  $\cdot\text{NO}$  in biological systems. Adapted from (Davis *et al.*, 2001).

## 2. The nitric oxide synthase (NOS)

$\cdot\text{NO}$  is produced *in vivo* by a family of nitric oxide synthase (NOS), a highly regulated enzyme that uses L-arginine (L-arg) and molecular oxygen ( $\text{O}_2$ ) as substrates. The three main isoforms: neuronal isoform (nNOS or NOSI), inducible (iNOS or NOSII) and endothelial (eNOS or NOSIII), are products of different genes and have different cellular localization, regulation, catalytic properties and sensitivity to inhibitors (Tatoyan and Giulivi, 1998). Both nNOS and eNOS are constitutively expressed and regulated by the concentration of calcium through interaction with calmodulin (Mungrue *et al.*, 2003). In turn, iNOS expression depends on immune stimulation and inflammation,

being independent of  $\text{Ca}^{2+}$  increases. The mitochondrial isoform (mtNOS) despite being a distinct isoform appears to be a variant of the neuronal isoform, resulting from post-transcriptional processing of RNA (Elfering *et al.*, 2002)

### 2.1. Reductase and Oxygenase Domains

NOS are dimeric enzymes, formed by two identical subunits, each one with two distinct domains (Figure 2):

**(A) reductase domain**, at carboxyl terminal, which connects two flavin cofactors (FMN, FAD) and NADPH co-substrate. FAD and FMN catalyze the transfer reactions from NADPH to the heme in the oxygenase domain of the opposite subunit of the dimer.

**(B) oxygenase domain**, at amino terminal, that contains the a heme group (protoporphyrin IX) and binding sites for (6R)-5,6,7,8-tetrahydrobiopterin ( $\text{H}_4\text{B}$ ) and the substrate L-arginine (L-arg).

Between the two domains there exists a binding site for calmodulin (CaM), which stabilizes the homodimer (MacMicking and Nathan, 1997). Dimerization increases NOS activity by creating high binding affinity sites for L-Arg and  $\text{BH}_4$ , removing the heme group from the solvent phase, and facilitating the flow of electrons between two domains, from FMN in the reductase domain, to the heme group in oxygenase domain (Crane *et al.*, 1999).

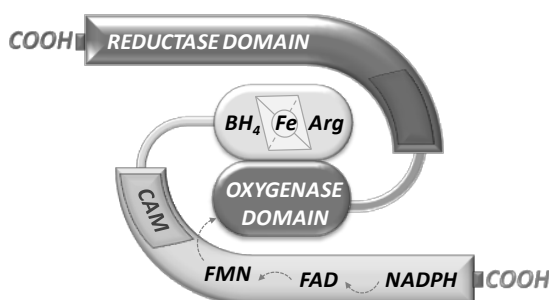
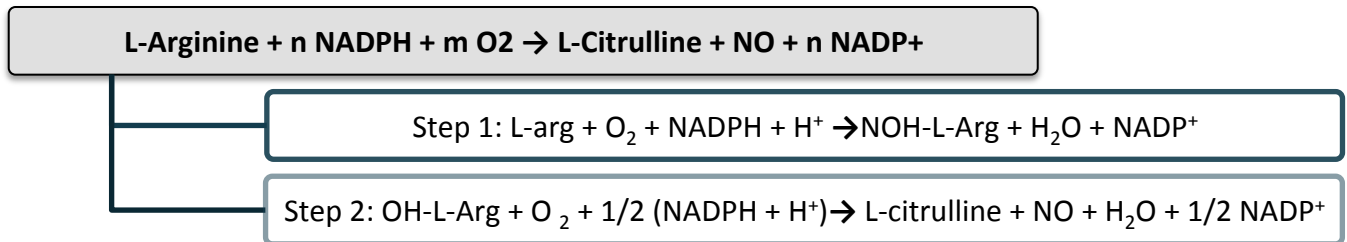


**Figure 2-** NOS structure indicating the oxygenase and reductase domain with binding sites for different cofactors, connected by a calmodulin (CaM) binding site. Adapted from (Cátia Lourenço, unpublished data).

## 2.2. 'NO Biosynthesis

In essence, 'NO derives from the oxidation reaction of L-arginine catalyzed by NOS to L-citrullin. The electrons flow from NADPH subunits to activate O<sub>2</sub> in the heme group of NOS, where L-Arg originates 'NO, L-citrullin and H<sub>2</sub>O, a reaction that occurs in two steps (Alderton *et al.*, 2001):

- a. L-arginine is hydroxylated to N<sup>ω</sup>-Hydroxy-L-arginine;
- b. N<sup>ω</sup>-Hydroxy-L-arginine is oxidized to 'NO and L-citrullin.



## 2.3. Regulation of nNOS

The NOS family is one of the most highly and complex regulated enzymes in Biology, involving transcriptional and post-transcriptional regulation, several substrates and co-factors, protei: protein interaction and subcellular localization.

The regulation of nNOS and subsequent 'NO bioactivity depends on several factors:

- Bioavailability of substrates (ex.: arginine) and cofactors (ex.: H<sub>4</sub>B and Ca<sup>2+</sup>/CaM) which are crucial for dimerization and activation of NOS, also applicable to eNOS (Jaffrey *et al.*, 1998);
- Concentration of intracellular Ca<sup>2+</sup> (Jaffrey *et al.*, 1998);
- Coupling of NMDA receptors to the enzyme (PSD-95), which regulates the subcellular localization of nNOS (Jaffrey *et al.*, 1998);
- Coupling of nNOS to different proteins, including CAPON, heat shock protein 90 (Bredl *et al.*, 1992), and phosphofructokinase (Firestein and Bredt, 1999), regulate their location.
- Phosphorylation of nNOS by protein kinases (which suggests that the synthesis of neuronal 'NO is modulated by a myriad of intracellular signaling cascades) (Bredl *et al.*, 1992);
- Binding of 'NO to the heme center to form a stable iron-nitrosyl (Fe<sup>2+</sup>-'NO), inactivating nNOS (Cooper, 1999).

### 3. Signaling pathways in central nervous system mediated by $\text{NO}$

$\text{NO}$  is present in virtually every area throughout the CNS and has been implicated in the regulation of diverse physiological functions such as visual information, learning and memory, motor planning, cognitive process that drives locomotion (Vincent, 2000), as well as in neurodegeneration. The mechanisms that support the wide range of effects of  $\text{NO}$  in central nervous system are still being clarified although it is well established that  $\text{NO}$  signaling in CNS is intimately associated to the glutamatergic system.

In glutamatergic synapses,  $\text{NO}$  synthesis involves the stimulation of ionotropic glutamate receptors, particularly NMDA-subtype to which nNOS is physically coupled, and influx of  $\text{Ca}^{2+}$  to the cytosol that, upon binding to calmodulin, activates the enzyme (Figure 3). Once produced, and considering  $\text{NO}$  reactivity with metal centers, it can control the activity of different heme proteins (sGC, NOS, catalase, cytochrome c oxidase) or non-heme (aconitase (Fe-S)), as well as regulate different cellular pathways via eNOS, with impact on physiology and pathology (Saran *et al.*, 1998).

In hippocampus, a brain region with crucial role in certain kinds of learning and memory processes,  $\text{NO}$  has been implicated in long-term potentiation (LTP), acting as a retrograde messenger and increasing the neurotransmitter release in the presynaptic nerve terminal (Mizutani *et al.*, 1993; Haley *et al.*, 1996; Prast and Philippu, 2001). The mechanism by which  $\text{NO}$  promotes neurotransmitter release is considered to be based on the activation of sGC, the best characterized signaling target for  $\text{NO}$ . The binding of  $\text{NO}$  to the heme of sGC promotes the activation of the enzyme that converts GTP in cGMP (Stone and Marletta, 1996). The cGMP produced, being a secondary intracellular messenger translates the  $\text{NO}$  signal into a cellular response, namely, activating cGMP-dependent protein kinases (Lucas *et al.*, 2000; Schlossman and Hofmann, 2005), which can regulate vesicle endocytosis (Micheva *et al.*, 2003) and thus modulate neurotransmission.

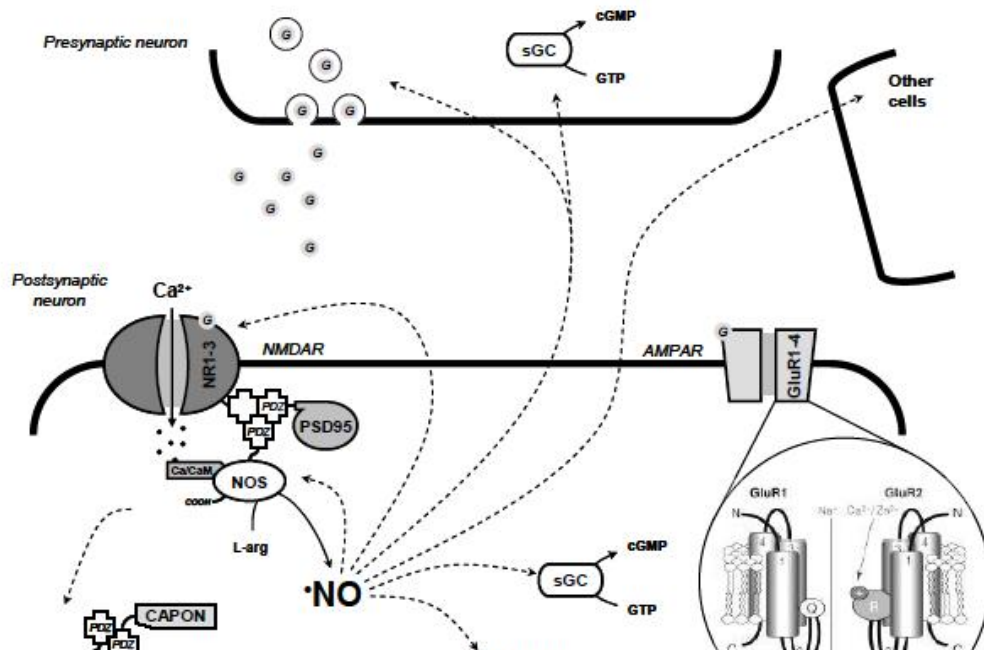


**Figure 3-** Glutamatergic synapse. Functional coupling between glutamate NMDA receptor with NOS, and signaling pathways mediated by nitric oxide. Adapted from (Frade, 2007).

Additionally, in hippocampus, NO has been implicated in neurodegeneration associated with Alzheimer disease (Contestabile *et al.*, 2003).

#### 4. Bioimaging of nitric oxide

While several techniques were developed to measure NO, the majority is based on indirect methods, not quantifying the radical per se, but instead the products of its decomposition or reaction with other molecules (Figure 4). An example of such technique is the Griess method, a colorimetric assay based on the measurement of nitrite, the oxidation product of NO. The test relies on the conversion of colourless sulphanilamide and N-(1-naphthyl)ethylenediamine to a purple azo dye (absorption peak 450 nm) through reaction with nitrite. However, this assay has serious drawbacks, inclusively the lack of sensitivity (LOD > 500 nM). In addition to the colorimetric methods, other methods have been applied to measure NO, such as chemiluminescence, Electron Paramagnetic Resonance (EPR) and fluorescence. Using chemiluminescence, NO can be quantified through reaction with ozone in the gas phase, leading to nitrogen dioxide in the excited state (Fontijn *et al.*, 1970), or by reaction with luminol-H<sub>2</sub>O<sub>2</sub> system in the liquid phase, generating a

chemiluminescent compound (Kikuchi *et al.*, 1993). Chemiluminescence has also gained recognition for measuring S-nitrosothiols and it is easily adapted to measure nitrite as a surrogate for  $\cdot\text{NO}$  generation; in this situation, the nitrite-containing sample is injected into an acid-containing mixture in order to generate  $\cdot\text{NO}$  for measurement (Pelletier *et al.*, 2006). By EPR  $\cdot\text{NO}$  can be measured, not directly (although it is a paramagnetic species it is too short-lived and has too broad spectrum to be detected satisfactorily by EPR), but through the use of spin traps, compounds that form paramagnetic adducts with  $\cdot\text{NO}$ , thus allowing the detection of this radical (Tsuchiya *et al.*, 2003). Other methodologies were developed allowing imaging  $\cdot\text{NO}$  in biological preparations based on the use of fluorescent compounds. One of the compounds most commonly used is the DAF-2 (4,5- diaminofluorescein), a compound that reacts with  $\text{N}_2\text{O}_3$ , an oxidation product of  $\cdot\text{NO}$ , giving rise to a highly composite fluorescent DAF-2T (triazolofluorescein) (Kojima *et al.*, 2001). This technique allows both the localization and quantification of  $\cdot\text{NO}$ , but it is limited to the requirement for higher oxides of nitrogen for activation (Suzuki *et al.*, 2002). Although valuable these methods are unable to reflect the  $\cdot\text{NO}$  concentration dynamics in tissues, as they are *ex situ* techniques, where the analysis is done out of the biological context and the measurements reflect  $\cdot\text{NO}$  concentration at a single time points. Therefore, and considering the previously described properties of  $\cdot\text{NO}$ , particularly that it conveys information through its concentration dynamics, direct detection of  $\cdot\text{NO}$  *in situ* is crucial for understanding its biological actions.

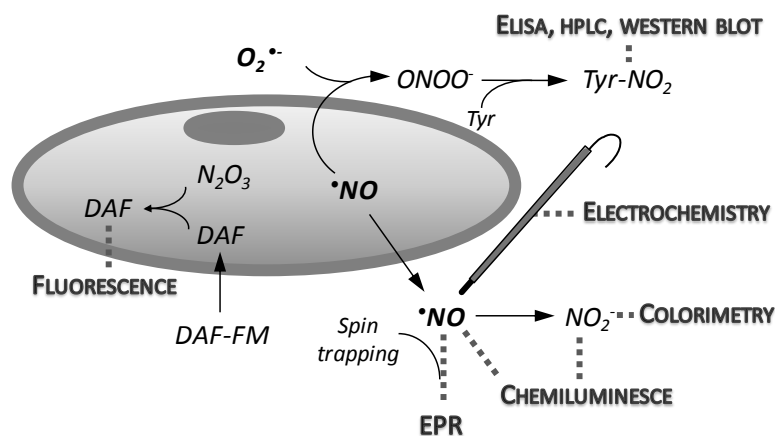


**Figure 4-** Techniques available for measurement of  $\cdot\text{NO}$  (Cátia Lourenço, unpublished data).

#### **4.1. Electrodes for $\text{NO}$ detection**

It is now generally accepted that electrochemical methods, particularly amperometry, associated to  $\text{NO}$  electrodes, is the only available technique that allow the direct and real time measurement of  $\text{NO}$  with enough sensitivity to detect relevant  $\text{NO}$  concentrations. Several electrodes for the direct electrochemical detection of  $\text{NO}$  have been developed, all based in the principle of  $\text{NO}$  reacting at an electrode to release electrons to the circuit, which can subsequently be measured as current. The earliest of these electrodes, known colloquially as the "Shibuki electrode", consists in a platinum (Pt) electrode covered with a gas-permeable membrane to successfully monitor endogenous  $\text{NO}$  production in rat cerebellar slices (Shibuki, 1991). However this sensor is reported to have limited biological usefulness, because it does not respond linearly to concentrations greater than  $1 \mu\text{M}$  and is subject to a destructive buildup of the oxidation products of  $\text{NO}$  within the enclosed electrolyte surrounding the Pt electrode. Nevertheless, it was an important hallmark because this probe enabled "World Precision Instruments" in 1992 to develop the first widely commercially available  $\text{NO}$  sensor, the ISO- $\text{NO}$ . A second hallmark in the development of sensors for  $\text{NO}$  detection was the introduction of catalytic electrode surfaces by Malinski and Taha, who used a metalloporphyrin membrane electrochemically deposited on a carbon fiber electrode (Malinski and Taha, 1992). Following this advance, the deposition of polymeric films that catalyse  $\text{NO}$  oxidation at the electrode surface became an attractive approach and several materials have been proposed, including different types of metalloporphyrins, metallophthalocyanines, copper-platinum microparticles, palladium and iridium oxide. However there are some concerns about the exact chemical mechanism by which these sensors detects  $\text{NO}$ , since carbon fibers without a porphyrin coating or with a coating of porphyrin without a metal ligand can also detect  $\text{NO}$  with significant sensitivity. Furthermore, because the surface of the electrode remained in direct contact with the measurement medium a variety of biological species were shown to interfere (i.e. give false responses) during  $\text{NO}$  measurement. Additionally, various other types of carbon fiber  $\text{NO}$  sensors that utilize a variety of different coating have been described, such as conducting and non-conducting polymers, multiple membranes, ruthenium, iridium and palladium, heated-denatured cytochrome c; Nafion<sup>®</sup>, o-phenylenediamine, polylysine, hemoglobin-DNA film and ionic polymers and  $\alpha$ -cyclodextrin (Bedioui and Villeneuve, 2003). Although the use of electrodes for  $\text{NO}$  detection can be endowed of some limitations, as potential

instability in biological medium and compromised selectivity against potential interferents, it has extraordinary advantages over almost all other methods of  $\text{NO}$  detection, not only because it allows the real time measurement *in situ* with minimal destruction, but also because of its high sensitivity (Megson and Miller, 2009, GMP book).

## II. Neurovascular coupling

Brain areas subject to increased neuronal activity consume increasing amounts of oxygen, glucose and other metabolites (Iadecola, 2004). This high energy consumption translates into higher consumption of ATP, essential for the operation of ( $\text{Na}^+/\text{K}^+$  and  $\text{Na}^+/\text{Ca}^{2+}$ ) pumps by maintain the gradient ion suitable for the generation of action potentials (mechanisms with higher energy costs), as well as the release of neurotransmitters (Drake and Iadecola, 2007). The brain being critically dependent on a continuous supply of blood, the blood flow required to accomplish these needs is ensured by a close link between neuronal activity and cerebral vasculature. This neurovascular coupling, characterized by increased blood flow that occurs when tissues are active in a given region, is called functional hyperemia, and its main goal is to regulate cerebral blood flow (CBF) with high spatiotemporal precision, towards maintain homeostasis (Hamel, 2006; Iadecola and Davisson, 2008, Leite *et al.*, 2009). Thus, the brain is an example of tissue that needs fuel more quickly or in larger quantities, possessing biological mechanisms for this complex and specialized neurovascular coupling, not only through direct interaction of neurons and vessels, but also involving astrocytes that may act as links between blood vessels and neurons (Zonta *et al.*, 2003). Therefore, these neurons are dependent on the hemodynamic response in the brain which is vital in supplying energy nutrients (glucose and oxygen) and residues removal from neuronal activity ( $\text{CO}_2$ , lactate excess, as well as other metabolites and heat) (Hossmann, 1994; Iadecola, 2004).

Such mechanisms result in an integrated action between neurons, glia, astrocytes and blood vessels (through the myocytes, endothelial cells and erythrocytes), indicating a close anatomical and functional link, the "neurovascular unit" (Figure 5) that acts by acting together, at cellular level to regulate local blood flow (Lo *et al.*, 2003; Iadecola and Davisson, 2008).



Biochemical and neural factors induce changes in blood vessels that result in changes in blood flow, volume and oxygenation. Although extensively investigated, this cascade of events is still poorly understood (Mesquita, 2009). The dependence of brain blood flow is enhanced by the fact that even relatively small reductions in cerebral blood flow (CBF) negatively affects neuronal function, particularly through the inhibition of protein synthesis. If large reductions in CBF occur, ATP synthesis is compromised, the brain cells reduce their ability to fire action potentials, and in severe cases the neurons undergo anoxic depolarization (missing gradient ion), leading to serious brain injuries and cerebral ischemia (Iadecola, 2004). Moreover, changes in blood vessels (ex.: caused by hypertension), by disrupting vessel regulatory mechanisms that ensure an adequate supply of blood in the brain, manifesting into disruption of control mechanisms, causing brain dysfunction and lead to various diseases, such as Alzheimer's, Parkinson's or other neurodegenerative diseases, cerebral ischemia or stroke. Thus, the investigation of neurovascular coupling is crucial to human health (Iadecola, 2004; Iadecola and Davisson, 2008).

## **1. Mechanism of neurovascular coupling**

It was proposed more than a century ago that neurons release vasoactive agents into the extracellular space that, subsequently, reach the blood vessels by diffusion leading to relaxation of vascular smooth muscle. Considerable evidences support the vasoactive neurotransmitters release, especially in the synaptic release of glutamate and GABA, but the mechanisms are much more complex and indirect than simple diffusion to vascular targets (Drake and Iadecola, 2007).

The exact mechanism behind the neurovascular coupling is currently under active investigation and discussion, however it is proposed that this coupling occurs not only indirectly through the astrocytic bridge, but also through direct interaction between vessels and neurons in glutamatergic synapses (Rossi, 2006; Drake and Iadecola, 2007, Stefanovic *et al.*, 2007). The current paradigm establishes an astrocytic bridge involving glutamate binding to metabotropic receptors on astrocytes (Rossi, 2006; Drake and Iadecola, 2007), allowing the (I) entry of calcium into glial cells, also from adjacent cells through gap junctions (GJ); (II)  $\text{Ca}^{2+}$  diffusion to the astrocytic feet, where it activates phospholipase A2 (PLA2); (III) release of arachidonic acid (AA) from phosphatidylinositol (PI); (IV) which is converted by cyclooxygenase (COX) into vasoactive prostanoids (particularly prostaglandin E2 (PGE2)). These prostanoids released by astrocytes play an important role in

regulating contraction and relaxation of smooth muscle, thus allowing greater blood flow when there is dilation. (Rossi, 2006; Drake and Iadecola, 2007).

While NO, a diffusible potent vasodilator and produced as a result of glutamatergic activation, has been suggested to mediate the neurovascular coupling, its role has been controversial. Recently, by simultaneously measuring NO dynamics and CBF and associated with a pharmacological screening, clear evidences were provided supporting a critical role of neuronal-derived NO in matching blood supply with neuronal activity in hippocampus. It was shown that NO released upon glutamatergic activation in neurons is able to diffuse to the nearby blood vessels, where by activating sGC, promotes vasodilation with consequent increase in CBF (Cátia Lourenço, unpublished data)

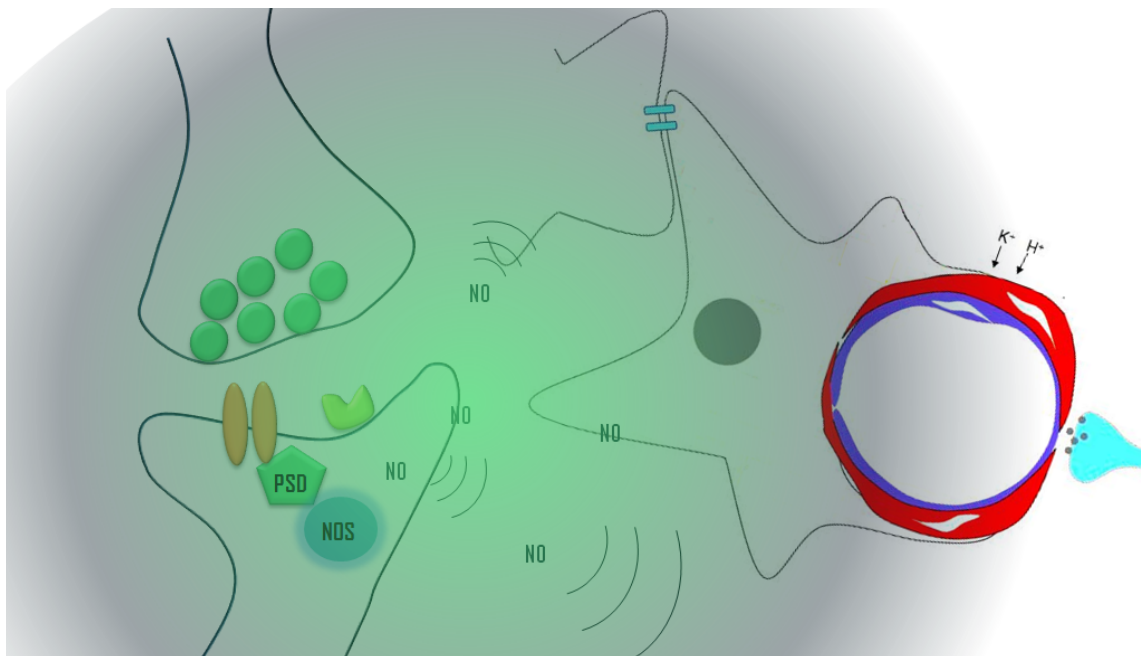


**Figure 5-** Neurovascular coupling mediated by isotropic diffusion NO. Adapted from (Drake and Iadecola, 2007).

### III. Alzheimer's disease

Alzheimer's disease (AD) is a complex and progressive neurodegenerative disorder associated to neuronal loss in brain areas linked to memory processing, in which  $\text{NO}$  has been implicated (Fernandez *et al.*, 2010).

In vulnerable brain regions, such as the hippocampus and cortex, there is an accumulation of extracellular neuritic plaques (deposits of differently sized small peptides called  $\beta$ -amyloid,  $\text{A}\beta$ , that are derived via sequential proteolytic cleavages of the amyloid precursor protein, APP) and intracellular neurofibrillary tangles (NFT) which consist largely of hyperphosphorylated twisted filaments of the microtubule-associated protein tau (Buee *et al.*, 2000; Gendron and Petrucelli, 2009), Proteolytic cleavage of APP in the amyloidogenic pathways mainly results in two forms of  $\text{A}\beta$ :  $\text{A}\beta_{40}$  [ $\text{A}\beta$ -(1–40)] and  $\text{A}\beta_{42}$  [ $\text{A}\beta$ -(1–42)] (Zhang *et al.*, 2010).

In spite of inconsistent results (Law *et al.*, 2001), all NOS isoforms are suggested to operate as central mediators of  $\text{A}\beta$  action, contributing to the maintenance, self-perpetuation and progression of the disease (Fernandez *et al.*, 2010).

During the development of AD it has been noticeable the neurotoxic effects of  $\text{NO}$  supported the pathological mechanisms involving its conversion to more reactive species, namely through the production of RNS and induction of nitrosative stress (due to indirect reaction of  $\text{NO}$ ). In addition to the ability of  $\text{A}\beta$  itself in generating oxidative stress (Varadarajan *et al.*, 2000), it can act synergistically with  $\text{NO}$  to induce neuronal damage. Concordantly, high levels of nitrotyrosine have been found in AD patients brains. Moreover, several studies have shown that important proteins are S-nitrosated in AD, such as PDI and dynamin. In addition, cerebrovascular dysfunction detected in AD may be important for the development of the disease, contributing to cognitive decline and neurodegeneration. Indeed, many patients with AD have regional cerebral hypoperfusion that correlates with cognitive decline (Chow *et al.*, 2007). Furthermore, fMRI studies have established that there is an increased delay in the CBF response in patients with increased cognitive impairment especially AD patients (Rombouts *et al.*, 2005). However,  $\text{NO}$  may have a protective role against the development of AD pathology. For instance, it was shown that  $\text{NO}$  derived from normal endothelium protects against increases in  $\text{A}\beta$ , by directly modulating levels of  $\text{A}\beta$ , APP and BACE-1 (Austin *et al.*, 2010).

Nowadays, several factors have been described to determine the induction of cerebrovascular damage in AD, including endothelial dysfunction promoted by nitro-oxidative stress (a term here used to incorporate the action of both, oxygen- and nitrogen-derived reactive species) (Hamel *et al.*, 2008), loss or abnormal cholinergic innervations of intracerebral blood vessels and accumulation of A $\beta$  on the cerebral blood vessels (cerebral amyloid angiopathy) (Bell and Zlokovic, 2009). However, it is still a matter of debate the pathologic importance of these cerebrovascular alterations and it is unclear whether they were a cause or a consequence of neuronal dysfunction and neurodegeneration (Iadecola, 2004).

## **1. Bacteria are powerful stimulators of inflammation and are amyloidogenic**

It is well known that several bacteria, upon interaction with the mammalian immune-system, induce chronic inflammation and amyloid deposition exacerbating AD. This conclusion is now supported by more than 20 epidemiological studies showing that individuals were protected from AD if they have been taking anti-inflammatory drugs (Veld *et al.*, 2000). Thus, brain inflammation could be induced by systemic administration of LPS mimicking AD. LPS produces a robust initial inflammatory reaction, the innate immune response, in peripheral organs and in the brain (Julius, 2009), leading to activation of microglia, neutrophil infiltration, and mRNA/protein expression of inflammatory mediators (Jeong *et al.*, 2010). A well-studied model of acute inflammation in rodents is the systemic administration of the bacterial inflammatory surface molecule lipopolysaccharide (LPS), a bacterial endotoxin followed by robust innate immune response in peripheral tissues and in the brain. LPS is used world wide in experimental and *in vivo* models of inflammation and amyloidosis (Veld, 2000). After its recognition by soluble or membrane-bound CD14, LPS binds its signaling receptor, toll-like receptor 4 (TLR-4) (Triantafilou and Triantafilou, 2005) expressed in multiple peripheral sites including brain microvasculature. This is followed by fast and transient release of pro-inflammatory cytokines to the circulation affecting all peripheral organs and the brain (Bosshart and Heinzemann, 2007). In connection with this notion, AD lesions are characterized by the presence of a series of inflammatory mediators including cytokines, chemokines, proteases, adhesion molecules, free radicals, pentraxins, prostaglandins, anaphylatoxins, and activated complement proteins (McGeer and McGeer, 2002).

Hereupon, bacteria and their toxins are powerful inducers of inflammatory cytokines and activators of the complement pathway (Fox, 1990). It has been known for almost a century that chronic bacterial infections are frequently associated with amyloid deposits in the infected tissues. LPS and bacterial cell wall peptidoglycan are highly resistant to degradation by mammalian enzymes and thus may provide a persisting inflammatory stimulus (Ohanian and Schwab, 1967)

## **2. Inflammation, NO and polyphenolic pathways**

Epidemiological studies have suggested that appropriate consumption of polyphenol-rich natural products may reduce the incidence of certain age-related neurological disorders, including Alzheimer's disease, and thus modulate multi-factorial events such as neuroinflammation, glutamatergic excitotoxicity, oxidative stress, and depletion of endogenous antioxidants. The beneficial effect has been attributable, at least in part, to their direct effect on blood vessels and in particular on endothelial cells. Indeed, polyphenols have been shown to activate endothelial cells to increase the formation of potent vasoprotective factors including NO and endothelium-derived hyperpolarizing factor (Schini-Kerth *et al.*, 2011).

Polyphenols, in virtue of the plethora of protective effects manifested in various experimental models and clinical trials, seem to be appropriate as dietary supplements for preventing the functional decline of organs with age (Magrone and Jirillo, 2011) by decreasing the risk of a range of diseases, including cardiovascular disease (CVD), certain forms of cancer (Kuriyama *et al.*, 2006) and neurodegenerative diseases. Flavonoids (a major class of polyphenols) have also been shown to exert beneficial cognitive effects and to reverse specific age-related neurodegeneration. Polyphenols, including curcumin, epicatechin, and procyanidins, have been proposed in the past to predominantly act via antioxidant activity. The tricyclic structure of the flavonoids determines antioxidant effects that scavenge reactive oxygen species and chelate  $Fe^{2+}$  and  $Cu^+$ , but recently it has becoming clear that polyphenols may participate in the redox modulation of cell functions, including enzyme inhibition and upregulation of antioxidant defenses via changes in gene expression upon interaction with redox-sensitive transcription factors (Katz and Doughty, 2011).

Recently, Han *et al.*, (2006) suggested that the neuroprotective action of various polyphenols could be mediated by the activation of common "receptor" binding sites particularly present at the level of the cellular plasma membrane in the rat brain. It is hypothesized that the binding

polyphenols (able to transverse the blood brain barrier-BBB) to this receptor may be associated with increased NO synthase activity in the brain. Prolonged action of polyphenols on its receptor could, however, lead to decreased receptor sensitivity and/or increased tolerance. Antioxidants are able to increase availability of biologicaly active NO resulting in a partial decrease of blood pressure. (Han et al., 2006; Schmitt and Dirsch, 2009; Galleano *et al.*, 2010).

The current awareness that oxidative stress plays a pivotal role in the pathophysiologic processes of vascular dysfunction resulted in several treatment strategies to alter ROS levels by decreasing production and/or increasing radical scavenging. Polyphenols appear to involve their interaction with cellular signaling pathways and related machinery that mediate cell function under both normal and pathological conditions. The figure below illustrate their interactions with two such pathways, the MAP kinase (ERK, JNK, p38) and PI3 kinase/Akt signaling cascades, that allow them to impact upon normal and abnormal cell function, thus influencing the cellular processes involved neurodegeneration. For example, their ability to activate ERK in neurons leads to a promotion of neuronal survival and cognitive enhancements, both of which influence the progression of Alzheimer’s disease, whilst ERK activation by polyphenols in vascular endothelial cells influence nitric oxide production and blood pressure (Vauzour *et al.*, 2010).

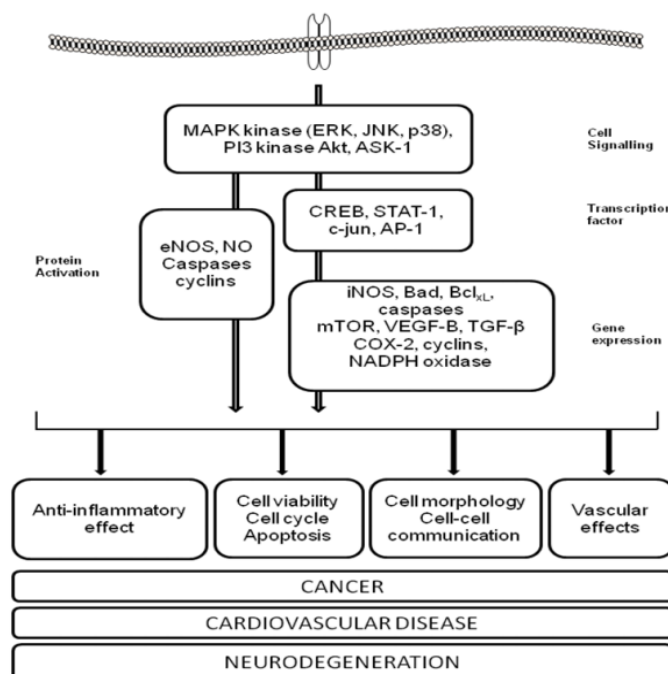


**Figure 6-** The interaction of polyphenols with cellular signaling pathways involved in chronic disease. Flavonoid-induced activation and/or inhibition of MAP kinase and PI3 kinase signaling leads to the activation of transcription factors which drive gene expression (Vazour *et al.*, 2010).

Polyphenols may act to protect the brain in a number of ways, including the protection of vulnerable neurons, the enhancement of existing neuronal function or by stimulating neuronal regeneration (Youdim and Joseph, 2001), to improve memory, learning and general cognitive ability (Vazour *et al.*, 2010). The effects of polyphenols on cognition and against neurodegenerative processes appear to be mediated via their interactions with neuronal and glial signaling pathways that affect gene expression and interfere with the cell death mechanisms (Williams *et al.*, 2004) directly via the inhibition of MAPK signaling cascades, such as p38 or ERK1/2. The effects of flavonoids on these kinases may influence downstream transcription factors, including nuclear factor-Kappa B (NF-κB). This suggests that there may be an interplay between signaling pathways, transcription factors and cytokine production in determining the neuroinflammatory response in the CNS (Figure 6). In this respect, the mechanisms by which polyphenols exert its beneficial function involve interactions with a number of cellular signaling pathways, which are important in the normal functioning of cells. Thus, polyphenols, in particular flavonoids, structurally resemble inhibitors of cell signaling cascades (MAPK/PI3).

Active flavonoid compounds were also found to inhibit <sup>1</sup>NO synthase activity of the three isoforms of the enzyme. It is hard to speculate on the broad ability of flavonoids to inhibit the activity of so many different enzyme systems but such inhibitors fit into the ATP binding pocket of the enzyme and it appears that the number and substitution of hydroxyl groups on the B ring and the degree of unsaturation of the C2-C3 bond are important determinants of this particular bioactivity (Spencer *et al.*, 2003). Yet, it is unlikely that the same three-dimensional orientation would be required by widely different enzymes. Another possibility is that flavonoids bind to proteins, thus changing their orientations and making their active site inaccessible (Middleton *et al.*, 2000).

## IV. Hypothesis

On basis of the beneficial and diverse effects of polyphenols in brain function, as well as their neuroprotective role against neurodegeneration and further considering that <sup>1</sup>NO produced in glutamatergic neurons diffuses isotropically until blood vessels leading to vasodilation, we

hypothesize that polyphenols, such as curcumin and epicatechin, by interfering with NMDA receptor:nNOS pathway, may modulate glutamate-induced  $\text{NO}$  concentration dynamics, thus affecting the neurovascular coupling.

Therefore, by simultaneously and in real time measuring  $\text{NO}$  dynamics and CBF, we propose to assess:

1) to what extent glutamate-induced  $\text{NO}$  dynamics and coupled cerebral blood flow changes are prone to modulation by polyphenols in physiological conditions;

2) whether glutamate-induced  $\text{NO}$  production is altered under pathological conditions, such as AD and inflammation, and whether the neurovascular coupling is compromised;

3) if polyphenols have any effect over  $\text{NO}$  dynamics and CBF under the previous mentioned pathological conditions.



Chapter 2.

# Materials and Methods



The feasibility of this approach is supported by the use of an array consisting of a microelectrode selective for  $\text{NO}$ , an ejection pipette and a laser Doppler flow probe to measure localized cerebral blood flow (CBF). Such an array will be stereotaxically inserted in the brain of the living rat and, upon glutamate stimulus in hippocampus and the dynamics of  $\text{NO}$  and of CBF will be measured in real-time and simultaneously (Figure 7).

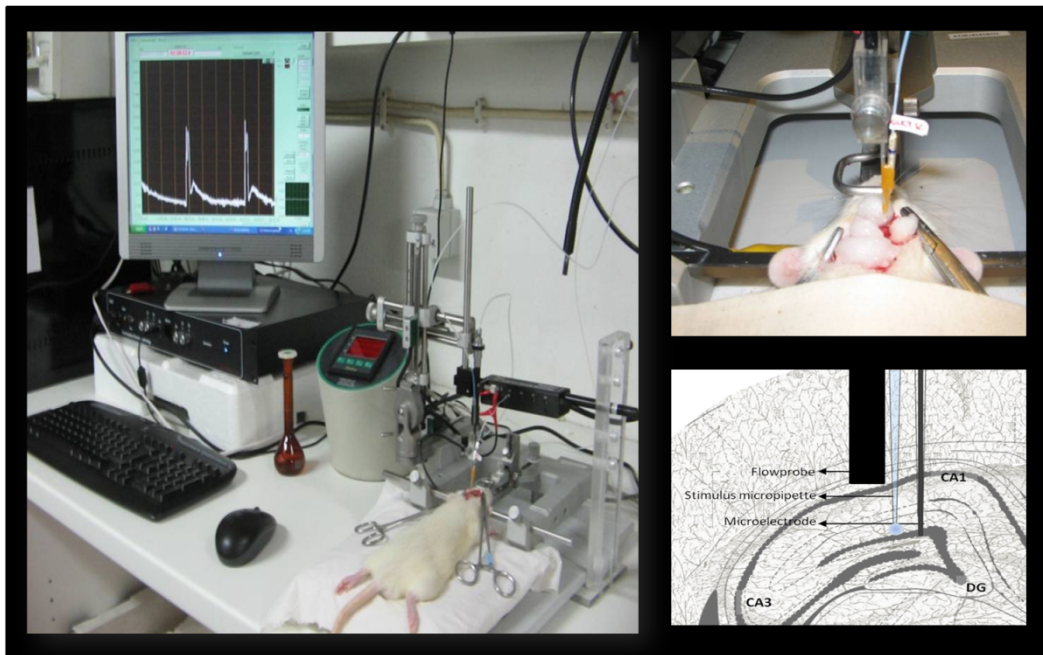


**Figure 7-** Measurement of CBF and  $\text{NO}$  on rat hippocampus. Array consists of a laser doppler probe for measure cerebral blood flow (CBF), a stimulus micropipette for glutamate injection, and a microelectrode to measure  $\text{NO}$  production.

## I. Experimental Design

To study the involvement of neurovascular coupling on brain inflammatory diseases mimicked by rat models of Alzheimer's Disease (comproved by behavioral tests) as well as administration of lipopolysaccharide (LPS) in male Wistar rats, the project was carried out *in vivo*, to establish potential physiological effects, as well as the modulation of dietary polyphenols in such dementia conditions.

## II. Chemicals and Solutions

Curcumin and (-)-Epicatechin and lipopolysaccharide (LPS) used in the study were purchased from Sigma. A $\beta$ <sub>1-42</sub> peptide was purchased from American Peptides. Ascorbate (AA) and o-phenylenediamine (o-PD) were obtained from Fluka. L-Glutamic acid (Glu) was purchased from Sigma and Nafion1 was purchased from Aldrich. Phosphate buffer (0.05 M PBS) used for microelectrode evaluations was prepared in MilliQ water and had the following composition (mM): 10 NaH<sub>2</sub>PO<sub>4</sub>, 40 Na<sub>2</sub>HPO<sub>4</sub>, and 100 NaCl (pH 7.4). All drugs ejected into the brain were dissolved in deoxygenated saline (NaCl 0.9%, pH 7.4). Ketamine (IMALGENE<sup>®</sup> 1000) and xylazine (Rompum 2%) were supplied by the Animal House of the Center for Neurosciences and Cell Biology (Coimbra). Urethane was purchased from Aldrich.

## III. *In vivo* testing

### 1. NO Microelectrodes

We use carbon fiber microelectrodes fabricated as described elsewhere (Santos, 2008). Briefly, single carbon fibers (30  $\mu$ m) were inserted into borosilicate glass capillaries and then pulled on a vertical puller. The salient carbon fibers were cut by tweezers under a microscope to obtain an exposed carbon surface with a tip length of 200 $\pm$ 50  $\mu$ m length.

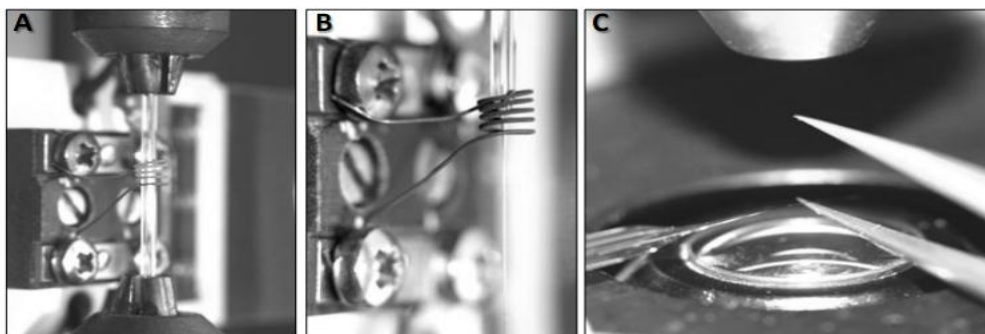


**Figure 8-** Microelectrodes fabrication (A-B) Pulling of the glass capillary with a carbon fiber inside in a vertical puller. (C) Cutting 200  $\pm$  50  $\mu$ m of fiber under the microscope (Cátia Lourenço, unpublished data).

Afterwards, a copper wire was introduced, followed by the introduction in the stem end of the microelectrode of conductive silver paint using a syringe, to provide the electrical contact between copper wire and the carbon fiber. The microelectrodes were tested for their general recording properties in phosphate-buffered saline (PBS) medium, by fast cyclic voltammetry (FCV) at a 200 V/s scan rate between  $-0.4$  and  $1.2$  V for 30 s. Finally, to improve their analytical properties for measuring  $\cdot\text{NO}$  in the rat brain *in vivo*, the carbon fiber microelectrodes were modified in a two-step protocol with Nafion<sup>®</sup> and *o*-PD. Nafion<sup>®</sup> coating was preformed by immersing microelectrodes tip in the Nafion<sup>®</sup> solution for 1-2 seconds and drying into an oven at  $170-180^{\circ}\text{C}$  for 4 min. The procedure was repeated twice. After Nafion coating, the *o*-PD layer was deposited by electropolymerization by placing the microelectrode tip in a 5 mM *o*-PD solution and applying a constant potential of 0.7 V vs an Ag/AgCl reference electrode for 30 min.

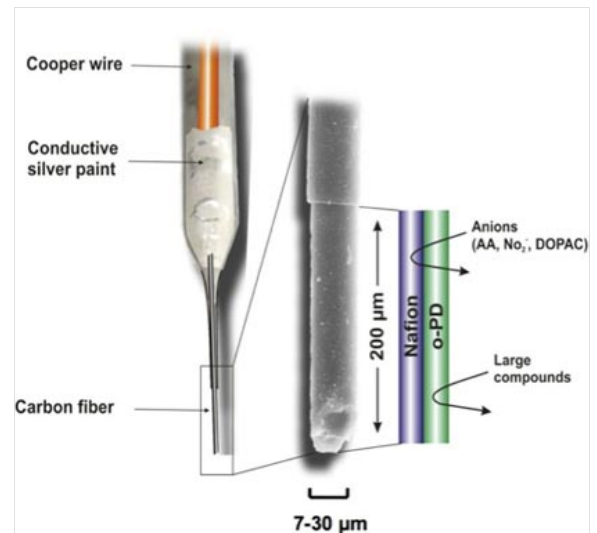


**Figure 9-** Schematic representation of exclusion layers of Nafion<sup>®</sup> and *o*-phenylenediamine at the carbon fiber surface. ([http://www.cnbc.pt/research/areaC1\\_2.asp?lg=2](http://www.cnbc.pt/research/areaC1_2.asp?lg=2)).

## 2. Calibration and Selectivity

The analytical performance of modified carbon fiber microelectrodes was assessed in terms of sensitivity, detection limit for  $\cdot\text{NO}$  and selectivity ratios against major interferents: ascorbate and nitrite (Ledo *et al.*, 2002).

Each microelectrode was calibrated with a fresh saturated solution of  $\cdot\text{NO}$  (prepared by bubbling  $\cdot\text{NO}$  gas in MilliQ water until saturation). Typically, the concentration of the saturated  $\cdot\text{NO}$  solution was *c.a.* 1.9 mM (Barbosa *et al.*, 2011) and was checked by ISO-NOP 2-mm Pt sensor connected to the amperometer ISO-NO Mark II, calibrated by chemical generation of  $\cdot\text{NO}$  from the reaction of  $\text{NO}_2$  with excess iodide and sulfuric acid (Mesaros *et al.*, 1997).

The calibration of the modified carbon fiber microelectrode was done by amperometry using the FAST-16 system with an applied potential of 0.9 V vs Ag/AgCl reference electrode. After

stabilization of background current for at least 20 min, the microelectrodes were calibrated. First, 250  $\mu\text{M}$  ascorbic acid (final concentration) is added and then, after current stabilization, three 10  $\mu\text{l}$  consecutive additions of  $\cdot\text{NO}$  solution are added with a gas-tight syringe in order to get a final concentration in the range of 0.4 to 2  $\mu\text{M}$ . Finally, nitrite was added at a final concentration of 100  $\mu\text{M}$  (Barbosa, *et al.*, 2008). A typical recording obtained with this procedure is shown in figure 10.

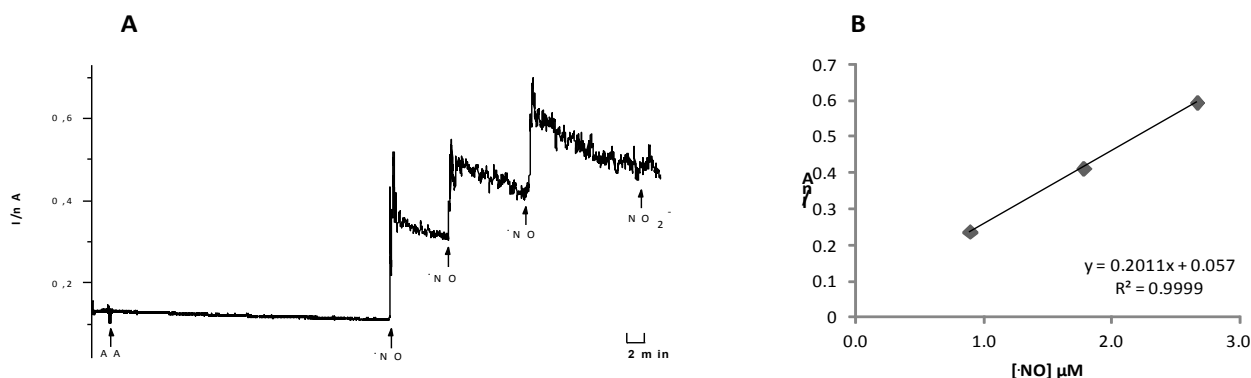


**Figure 10-** Determination of microelectrodes sensitivity for  $\cdot\text{NO}$  and selectivity against interferences. (A) Representative recording of microelectrode calibration. Compounds were added at the times indicated by the upper arrows. (B) Linear regression applied to the correlation between the concentration of  $\cdot\text{NO}$  added and the current change resulting from each addition.

The calibration parameters calculated for  $\cdot\text{NO}$  are the slope (sensitivity), limit of detection (LOD), and linearity ( $R^2$ ). The LOD is defined as the analyte concentration that yields an electrode response equivalent to three times the background noise of the recording system.

Selectivity ratio ( $\cdot\text{NO}$  vs interferences) is calculated as the ratio of microelectrode sensitivity for  $\cdot\text{NO}$  over interferences and is calculated by dividing the  $\cdot\text{NO}$  slope by the interferent slope.

The properties of the chemically modified carbon fiber microelectrodes used are summarized in table 1.

**Table 1-** Calibration parameters and selectivity ratios of carbon fiber microelectrodes coated with Nafion and o-PD. (Data are given as mean $\pm$ SEM).

Sensitivity ( pA/ $\mu\text{M}$ )	304 $\pm$ 28 (n=16)
Linearity ( $R^2$ )	0.998 (n=16)
Detection limit (nM)	8.910 $\pm$ 28 (n=16)
Selectivity ratio	
Ascorbate	9452 $\pm$ 2293 : 1 (n=16)
Nitrite	2813 $\pm$ 753 : 1 (n=16)

## 2.1. Neurodegenerative rat models

### *Acute model of AD*

The brain AD of rat as well as the memory impairment was developed by a single intracerebroventricular injection of A $\beta$  peptide (fragment 1-42) in rat brain, accordingly to a previously described procedure (Canas *et al.*, 2009). Male rats were anaesthetized with a mixture of ketamine 4:1 xylazine (2,5 mg/Kg, IP), and underwent a intracerebroventricularly (ICV) infusion at a rate of 0.2  $\mu$ l each 20 seconds of 4  $\mu$ l of A $\beta$ -amyloid (1-42) (2.257 mg/ml) into the right lateral ventricle, using stereotaxic coordinates: anterior-posterior (AP)- 0.8; medial-lateral (ML)-1.5; dorsoventral (DV)-3.5, according to the atlas of Paxinos and Watson (2007), by microlitre syringe (Hamilton) as previously described (Dall'igna *et al.*, 2007). Control animals were ICV injected with a similar volume of saline. At the end of the infusion the rat's scalp was sutured. Animals were allowed to recover and tested after 15 days for behavioral performance. *In vivo* recordings were performed 18-19 days after A $\beta$  infusion.



**Figure 11-** (A) AD induction by intracerebroventricular injection of A $\beta_{1-42}$ . (B-C) Anesthetic recuperation after surgery, and in detail rat's scalp sutured.

### *Inflammatory Animal Model*

Additionally, an acute inflammatory brain model was induced by bacterial endotoxin lipopolysaccharide (LPS from *Escherichia coli*, serotype 0127:B8). Wistar rats were injected intracerebroventricularly (ICV) with LPS (20 µg dissolved in 4 µL of 0.9% NaCl), and in another set of experiments rats were pretreated with a single intraperitoneal injection of LPS (2 mg/kg).

## **3. Behavior Tests**

Behavior tests were performed to address whether the AD models used in this work presented cognitive deficits that resemble those known to exist in AD, namely by related to novelty and memory. Each behavioral test was performed in an isolated room with lighting conditions and environmental cues held constant throughout testing. Animals were delivered to the experimental room the day before the experiment. All behavioral tests were carried out between 10 p.m and 4 p.m, under red-light illumination. To remove the smell traces left by the animals, before each trial the surfaces of the arenas, maze and objects were carefully cleaned. All behavioral tests were carried out between 10 p.m and 4 p.m.

### ***3.1. Open field***

The open field locomotion test is primarily used to examine motor function by means of measuring spontaneous activity and exploratory behaviors in an open field arena (Denenberg, 1969). Animals were placed in an open field arena (75x60 cm, divided in 20 squares of 15 cm) for 10 minutes and the total number of line crossings (horizontal explorations) and the number of rearings (vertical explorations) were counted.

### ***3.2. Novel-Object recognition test***

The object recognition test is based on the natural tendency of rodents to investigate a novel object instead of a familiar one (Squire *et al.*, 2007). In this task, animals were placed in an open field arena (75 x 60 cm) with two identical objects for 5 minutes, during which the animal has habituated to the configuration and properties of the different objects. After 2 hours, animals were

placed in the same arena in which one of the objects was replaced by a new one, with different configuration and color, and left there for 5 minutes. In each trial, the time spent inspecting each object was measured. The index of novel object recognition was calculated as the percentage of time spent inspecting the novel object.

### **3.3. Y-maze**

Another recognition memory test was carried out in a Y-maze apparatus. The Y-maze is constituted by 3 equal arms with an angle of 120 degrees between them. In a first trial, animals were placed in the Y-maze with an arm blocked and the animals were allowed to explore the two arms for 5 min. After 2 hours, the animals were placed back into the maze, this time with all arms open, and scored for 5 minutes. The number of entries and the time spent in each arm were recorded. The percentage of time spent in the novel arm was used as index of cognitive function.

## **4. Array production**

For the simultaneous measurement of NO and CBF the micropipette is attached to the carbon fiber microelectrode using sticky wax, that has been softened by flame. The precise placement is done using a microscope fitted with a reticule to achieve a distance between the tip of the micropipette and the NO microelectrode of  $250 \pm 50 \mu\text{m}$ . Laser Doppler probe is finally attached to microelectrode-micropipette array around  $500 \mu\text{m}$  back from the tip.

## **5. Animals and surgical preparation**

*In vivo* studies were carried out in adult male Wistar rats (8–10 week, weighing 290–350 g) there were maintained in our own animal facilities under controlled environment ( $23 \pm 2^\circ\text{C}$ , 12 h-light/dark cycle, free access to food and water). Experiments were performed in accordance with the European Community Council Directive for the Care and Use of Laboratory Animals (86/609/ECC) and were approved by the local institutional animal care committee. Institutional guidelines were followed during entire experimentation.



For *in vivo* studies, rats were anesthetized with urethane (1.25–1.50 g/kg, IP) and placed in a stereotaxic frame (Stoelting, USA) on an isothermal pad to maintain its body temperature at 37°C (Burmeister *et al.*, 2002).

After exposing the surface of the skull, a small hole was drilled above the recording area and dura matter removed gently to expose the brain surface. An Ag/AgCl reference electrode previously prepared is introduced in the brain. Brain surface was bathed with saline (0.9% NaCl) to prevent drying of the brain surface. The array consisting in the microelectrode-micropipette-LDF probe was then inserted into the rat hippocampus using a hydraulic micromanipulator, using the following coordinates, calculated from bregma (0,0,0) based on the rat brain atlas of Paxinos and Watson (2007): AP- 4.1; ML- 1.5; DV- 3.7.

## **6. Stimulation and pharmacological modulation of $\cdot$ NO with Curcumin and Epicatechin**

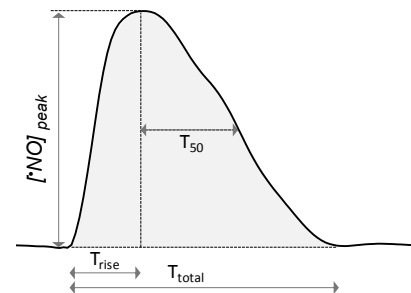
After the insertion of the array into the hippocampus, the baseline current stabilize for at least 30 min. Then  $\cdot$ NO production was stimulated by ejection of L-glutamate from a micropipette using a Picospritzer III (Parker Hannifin, General Valve Operation, USA), using pressure pulses for 1 s at 7–15 psi. L-glutamate solution 20 mM was prepared in NaCl 0.9%. The volume ejected (low nanoliter range) was calculated by the decrease of the volume of the micropipette measured through a stereomicroscope (Meiji EMZ 13, Japan) fitted with an eyepiece reticule.  $\cdot$ NO production was modulated with curcumin, and epicatechin. Rats were treated with a single dose (acute administration) of 300mg/kg of curcumin emulsified in dimethyl sulfoxide (DMSO) intraperitoneally or intraventricularly at a concentration of 20 mM  $\mu$ L dissolved in 1 $\mu$ L of DMSO. To examine the neuromodulatory effect of curcumin and epicatechin in terms of neurovascular coupling, we will measure the  $\cdot$ NO levels and CBF in rats before administration of this dietary phenols (control), regardless the route of administration after supplementation.

## **7. Data analysis**

The characterization of *in vivo* signals was assessed by electrochemical and pharmacological verification, and were individually analyzed using the OriginPro 7.5 Software, accordingly to the example depicted in Figure 12. Briefly, the individual  $\cdot$ NO signals were characterized in terms of 1)

[NO] peak, the peak concentration of the signal; 2) *area*, calculated as the time integral of the signal; 3)  $T_{rise}$ , the time in seconds necessary to reach the maximum amplitude after the application of the stimulating solution, 4)  $T_{50}$ , the time in seconds from maximum amplitude to 50% decay of the signal, 5)  $T_{total}$ , the time in seconds from the application of the stimulation to return to basal levels and 6) *Half Width (dx)* time by which amplitude reaches half of the maximum levels (Barbosa *et al.*, 2008).

**Figure 12-** Schematic diagram of a 'NO signal to illustrate how signal parameters were measured and calculated, namely the [NO] peak, area (shaded),  $T_{rise}$ ,  $T_{50}$  and  $T_{total}$ .



Records from CBF were exported from the Perisoft version 2.50 software, averaging 1 point per second, and synchronized with 'NO recorded dynamics based on the markers recorded at the time of stimulations. CBF changes were analyzed in terms of 1) *Basal levels*, perfusion values previous to stimulation; 2) *CBF change*, relative change in CBF in respect to the basal levels (percentage), 3)  $T_{rise}$ , the time in seconds necessary to reach the maximum amplitude after the application of the stimulating solution; and 4)  $T_{total}$ , the time in seconds from onset to return to basal levels. Additionally, the delay time of the onset and peak between both dynamics was determined. All statistical analyses were performed using GraphPad Prism 5 Software. Data are presented as mean  $\pm$  SEM. Statistical analyses of the data were performed using one-way analysis of variance (ANOVA) followed by post-hoc Bonferroni's Multiple Comparison Tests or a Student's t-test. Differences were considered significant at  $p < 0.05$ .

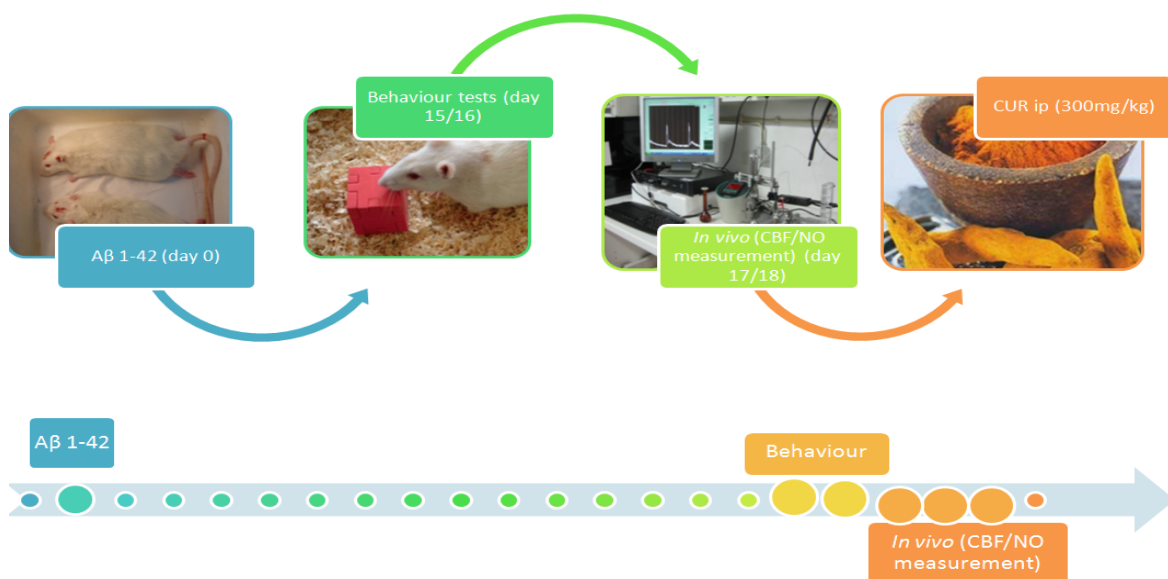
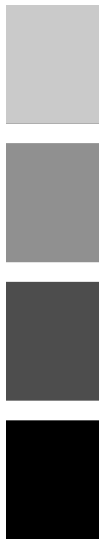


**Figure 13-** Experimental Schedule.

Chapter 3 .

# Results



## I. *In vivo* Nitric Oxide and cerebral blood flow coupling dynamics

As previously reported, a localized stimulation with glutamate in rat hippocampus promotes an instantaneous and transient elevation of  $\cdot\text{NO}$  concentration levels (Lourenço *et al.*, 2010) that in turn is followed, seconds later, by an also transient increase in CBF (Cátia Lourenço, unpublished data).

In figure 14, is shown a typical set of  $\cdot\text{NO}$  and CBF signals recorded in rat hippocampus upon sequential stimulations with 15-min intervals with L-glutamate (20 mM, 25 nL, 1s). For this particular record, the  $\cdot\text{NO}$  production was characterized by a maximal peak  $\cdot\text{NO}$  concentration increase ranging from 1.3 to 0.7  $\mu\text{M}$ , with an average duration of 56 s. The CBF started to increase with an average of 3 s after stimulation, reaching 94 % of the basal level after 39s and returning to baseline after 437 s.

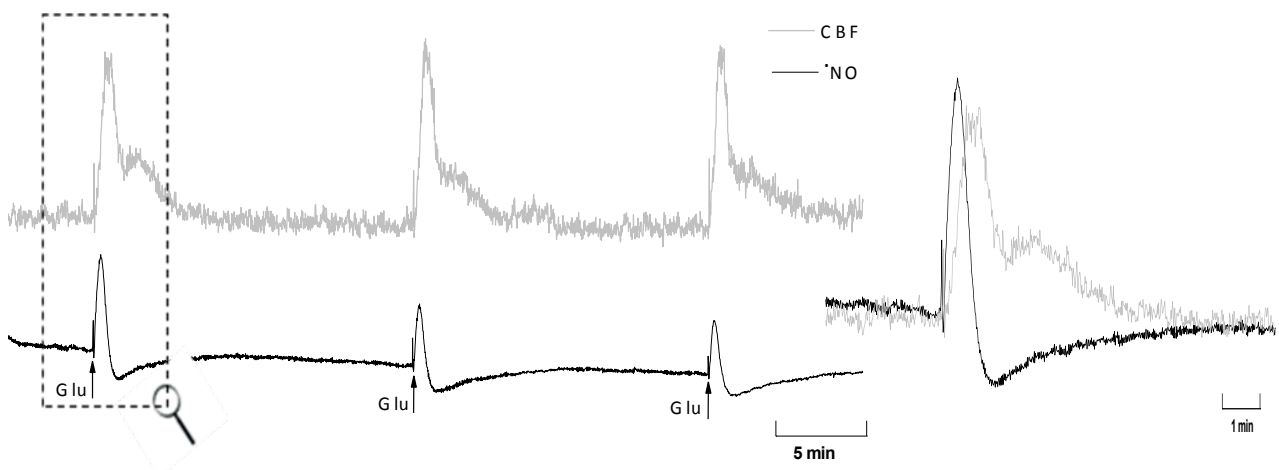


**Figure 14-** Representative recording of the simultaneous measurements of  $\cdot\text{NO}$  produced by local application of L-glutamate on rat hippocampus (bottom, black line) and CBF changes (top, light grey line). L-Glutamate (20 mM, 25 nL) was locally applied at times indicated by the arrows.

## II. Modulation of neuronal-derived $\text{NO}$ and neurovascular coupling with Polyphenols

Several lines of evidence suggest the beneficial role of dietary polyphenols by ameliorating brain function and protecting against neurodegeneration. Polyphenols neuroprotection has been ascribed to direct radical scavenging/antioxidant activity, but most significantly by modulation of signaling pathways with significance in cell survival and death (Frade *et al.*, 2005). Based on the above mentioned, it was pertinent to address the potential of polyphenols to modulate glutamate induced  $\text{NO}$  production and cerebral blood flow.

Among a wide variety of polyphenols to which a plethora of protective effects in several experimental models were described, we selected curcumin, the yellow pigment of the widely used spice, turmeric, and epicatechin, a flavanol found, for instance, in green tea, grapes and blueberries. Both were reported to permeate the blood brain barrier and modulate important signaling pathways in the brain (Frade *et al.*, 2005; Lin, 2007; Van Praag *et al.*, 2007).

### 1. Curcumin

The endogenous  $\text{NO}$  production induced by activation of glutamate receptors and dependent neurovascular coupling was acutely modulated by curcumin via two distinct routes of administration: i) intracerebroventricular (ICV) and 2) intraperitoneal (IP) injection. In order to maximize the reproducibility of the effects, curcumin was only injected after obtaining 2-3 consecutive signals with similar amplitude. Figure 15 shows a typical recording of the effect of curcumin administered ICV (20 mM) in  $\text{NO}$  production and CBF induced by L-glutamate in hippocampus. The parameters obtained by the analysis of individual  $\text{NO}$  peaks and CBF changes before and after curcumin administration are summarized in the Figure 16 and detailed table 2. Globally, we observed that curcumin, once administered ICV, promoted a slight decrease of glutamate-induced  $\text{NO}$  production, particularly significant regarding the duration of  $\text{NO}$  concentration dynamics. The reproducibility of the  $\text{NO}$  signals obtained with repeated stimulations with L-glutamate prior to curcumin administration strengthens the observation that the decrease in  $\text{NO}$  signals is likely due to curcumin. In detail, approximately 20 min after the ICV injection of curcumin glutamate-induced  $\text{NO}$  signals showed decreased amplitude (19%, n=7), as well as

duration (29%,  $p < 0.05$ ). Coherently with the idea that  $\cdot\text{NO}$  mediates the neurovascular coupling in hippocampus, the CBF changes coupled to  $\cdot\text{NO}$  dynamics also appeared slightly reduced after curcumin ICV administration (CBF change associated to glutamate stimulation after curcumin was 25.06% reduced as compared to control levels).

Consistently with the idea that  $\cdot\text{NO}$  mediates the neurovascular coupling in hippocampus, the CBF changes coupled to  $\cdot\text{NO}$  dynamics also appeared reduced after curcumin ICV administration, although not significantly (CBF change associated to glutamate stimulation after curcumin was 10% reduced as compared to control levels).

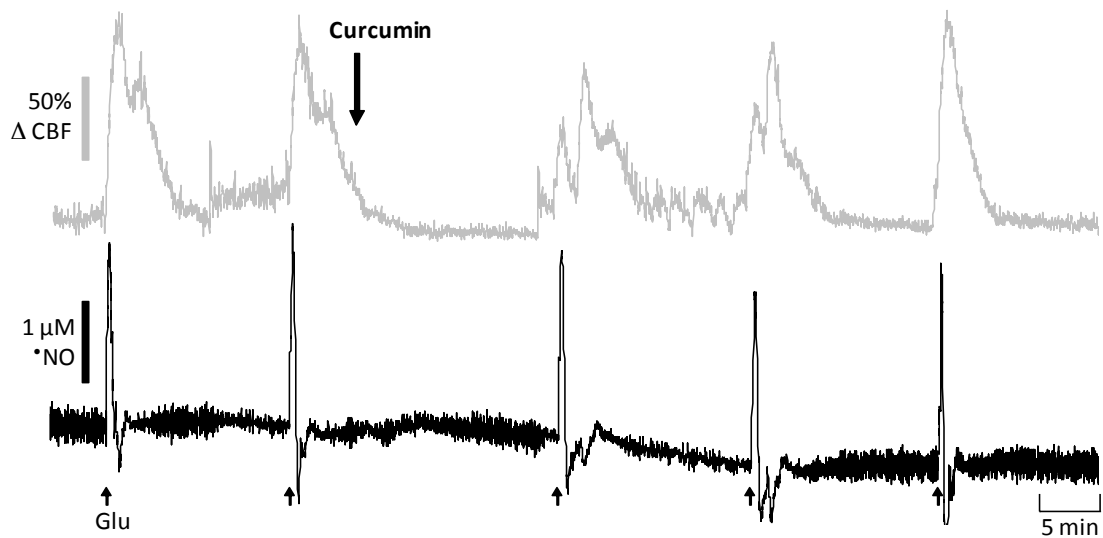


**Figure 15-** Effect of curcumin in glutamate-induced  $\cdot\text{NO}$  dynamics (black line) and CBF changes (grey line) in rat hippocampus. L-Glutamate (20 mM, 25 nL) was locally applied at times indicated by the upward arrows. Curcumin was intracerebroventricularly administrated (20 mM) at the time indicated by the downward arrow.

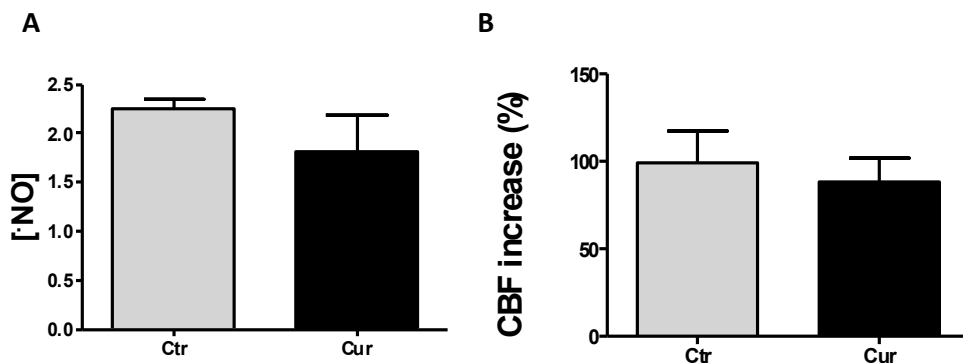


**Figure 16-** Quantitative analysis of peak  $\cdot\text{NO}$  concentrations (A) and CBF amplitude (B) before and after curcumin intracerebroventricular injection. Data represents mean  $\pm$  SEM. Statistical analysis was performed by Student's t-test in relation to control experiments ( $*p < 0.05$ ).

**Table 2-** Analysis of glutamate-induced  $\dot{\text{NO}}$  signals and CBF changes in hippocampus before and after curcumin injected in intracerebroventricularly.

	Ctrl (n= 2)	Cur (n=4)	P	
$\dot{\text{NO}}$	[ $\dot{\text{NO}}$ ] peak ( $\mu\text{M}$ )	2.25 $\pm$ 0.10	1.82 $\pm$ 0.36	0.4733
	Trise (s)	17 $\pm$ 3	18 $\pm$ 1	0.3726
	Ttotal (s)	49 $\pm$ 8	35 $\pm$ 4	0.0103*
	Half width (s)	20 $\pm$ 3	16 $\pm$ 2	0.0154*
CBF	CBF increase (%)	100 $\pm$ 17.5	90 $\pm$ 16	0.6582
	Trise (s)	56 $\pm$ 8	62 $\pm$ 28	0.3726
	Ttotal (s)	374 $\pm$ 10	352 $\pm$ 52	0.6595

Data represents mean $\pm$ SEM.

As previously mentioned, the effect of curcumin over  $\dot{\text{NO}}$  concentration dynamics and coupled CBF changes was further addressed by using intraperitoneal injection as administration route. The effects of curcumin administrated systemically (300 mg/kg) are summarized in figure 17 and detailed in Table 3. Contrary to the effect observed after ICV injection, curcumin injected IP had no significant effect either at the level of  $\dot{\text{NO}}$  production or CBF. Although a slight decrease was observed regarding the duration of  $\dot{\text{NO}}$  signals (19%, 9 peaks analyzed from 2 individual experiments),  $\dot{\text{NO}}$  peak concentration increased after curcumin intraperitoneal injection (15%). The glutamate-induced CBF increase was also slightly higher after curcumin injection (12%).

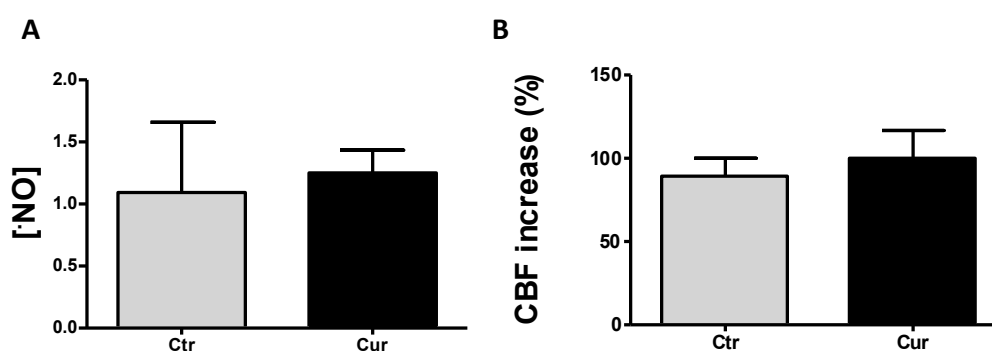


**Figure 17-** Quantitative analysis of peak  $\dot{\text{NO}}$  concentrations (A) and CBF amplitude (B) before and after curcumin intraperitoneal injection. Data represents mean  $\pm$  SEM. Statistical analysis was performed by Student's t-test in relation to control experiments (\* $p < 0.05$ ).

**Table 3-** Analysis of glutamate-induced  $\cdot\text{NO}$  signals and CBF changes in hippocampus before and after curcumin intraperitoneal injection.

		Ctr	Cur	P
		(n= 5)	(n=9)	
$\cdot\text{NO}$	[ $\cdot\text{NO}$ ] peak ( $\mu\text{M}$ )	1.09 $\pm$ 0.56	1.25 $\pm$ 0.19	0.7537
	Trise (s)	69 $\pm$ 28	52 $\pm$ 18	0.6188
	Ttotal (s)	137 $\pm$ 23	112 $\pm$ 24	0.4927
	Half width (s)	98 $\pm$ 19	76 $\pm$ 22	0.5124
CBF	CBF increase (%)	89 $\pm$ 11	100 $\pm$ 18	0.6834
	Trise (s)	96 $\pm$ 18	94 $\pm$ 18	0.9292
	Ttotal (s)	367 $\pm$ 53	293 $\pm$ 51	0.3780

Data represents mean $\pm$ SEM.

## 2. Epicatechin

The effects of epicatechin over neurovascular coupling mediated by  $\cdot\text{NO}$  were also evaluated by ICV injection. A representative recording of the effect of epicatechin 100  $\mu\text{M}$  over  $\cdot\text{NO}$  and CBF dynamics in hippocampus is shown in figure 18. The parameters obtained by the analysis of individual  $\cdot\text{NO}$  peaks and CBF changes before and after epicatechin administration are detailed table 4.

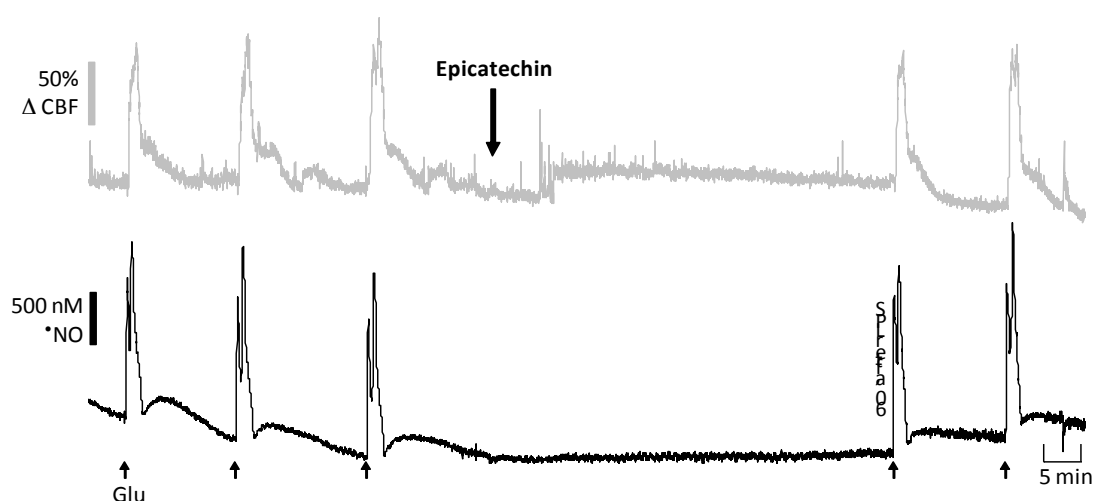


**Figure 18-** Effect of epicatechin in glutamate-induced  $\cdot\text{NO}$  dynamics (black line) and CBF changes (grey line) in rat hippocampus. L-Glutamate (20 mM, 25 nL) was locally applied at times indicated by the upward arrows. Epicatechin (100  $\mu\text{M}$ ) was injected intracerebroventricularly at the time indicated by the downward arrow.



**Table 4-** Analysis of glutamate-induced  $\dot{\text{NO}}$  signals and CBF changes in hippocampus before and after Epicatechin (100 $\mu\text{M}$ ) locally applied in hippocampus.

	Ctrl (n= 3)	Epicatechin 100 $\mu\text{M}$ (n=7)	P	
$\dot{\text{NO}}$	[ $\dot{\text{NO}}$ ] peak ( $\mu\text{M}$ )	1.62 $\pm$ 0.05	1.72 $\pm$ 0.11	0.4072
	Trise (s)	51 $\pm$ 4	52 $\pm$ 6	0.8953
	Ttotal (s)	135 $\pm$ 3	120 $\pm$ 7	0.3372
	Half width (s)	70 $\pm$ 1	73 $\pm$ 3	0.4072
CBF	CBF increase (%)	106 $\pm$ 10	112 $\pm$ 19	0.7780
	Trise (s)	82 $\pm$ 9	68 $\pm$ 3	0.3181
	Ttotal (s)	402 $\pm$ 16	356 $\pm$ 46	0.3372

Data represents mean $\pm$ SEM.

While in control conditions, average  $\dot{\text{NO}}$  peak concentration was  $1.62 \pm 0.05 \mu\text{M}$  and CBF change  $106 \pm 10\%$ , after epicatechin  $\dot{\text{NO}}$  peak concentration was  $1.72 \pm 0.11 \mu\text{M}$  and the CBF change  $112 \pm 19\%$ . Although without statistical significance, a slight increase (*c.a.* 6%) was observed in both  $\dot{\text{NO}}$  peak concentration and amplitude of CBF changes, as evidenced in figure 19. As previously observed for curcumin, a slight decrease was also observed regarding the duration of both  $\dot{\text{NO}}$  concentration dynamics and CBF changes after epicatechin ICV injection (*c.a.* 11%).

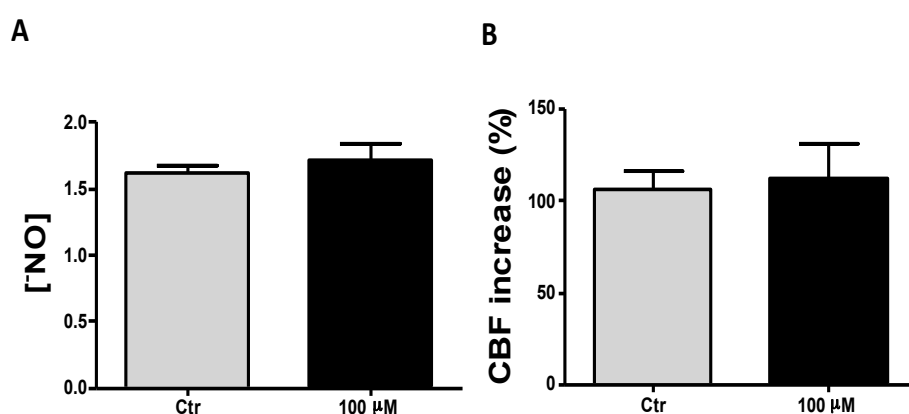


**Figure 19-** Quantitative analysis of peak  $\dot{\text{NO}}$  concentrations (A) and CBF amplitude (B) before and after Epicatechin (100  $\mu\text{M}$ ) intracerebroventricular injection. Data represents mean  $\pm$  SEM. Statistical analysis was performed by Student's t-test in relation to control experiments ( $*p < 0.05$ ).

In addition to the effect over glutamate-induced responses, it was interesting to note that the administration of epicatechin promoted an increase in basal CBF levels. As can be observed in figure 18, around 8 min after the injection of the polyphenol CBF increase, reaching a plateau 25% higher that was maintained till the following glutamate stimulation, after which the CBF basal levels were restored.

### 3. Discussion

NO, a free radical messenger produced upon glutamatergic neuronal activity in brain by nNOS, is implicated both in mechanisms of synaptic plasticity, underlying learning and memory, but also in neuronal degeneration. Because NO is highly diffusible and overcomes specific receptor interaction, it conveys information associated with its concentration dynamics, which implies that it is critical to measure directly NO concentration profiles to unravel its involvement in physiological and pathological processes. Recently, by measuring simultaneously NO and CBF changes, NO was identified as the mediator of the neurovascular coupling in rat hippocampus, establishing a diffusional wireless connection between active glutamatergic neurons and blood vessels (unpublish data). In this work, by using an identical approach we observed that localized glutamate injection in rat hippocampus results in transient elevations of NO levels, which are followed by transient increases in CBF. This observation corroborates the idea that NO match local blood supply with neuronal activity, a critical mechanism for the brain to maintain its structural and functional integrity (Drake and Iadecola, 2007).

Given that natural occurring polyphenols have been described to improve memory, learning and general cognitive ability as well as to afford neuroprotection against brain injury and neurodegeneration (Frade *et al.*, 2005), in this work, we addressed the potential of two polyphenols, curcumin and epicatechin, to modulate glutamate-elicited NO production and coupled cerebral blood flow changes. In addition to their antioxidant activity (Natsume, 2003, Münzel *et al.*, 2010), both curcumin and epicatechin has been shown to modulate several signaling pathways with significance in the context of this work. For instance, curcumin showed to protect against quinolinic acid-induced excitotoxicity in cultured neurons, by inhibiting the quinolinic acid-induced Ca<sup>2+</sup> influx and nNOS activity and to be a potent inhibitor of iNOS (Lin, 2007).

By simultaneous measuring NO concentration dynamics and CBF changes before and after an acute administration of curcumin intracerebroventricularly, we observed that it was able to

promote a slight decrease either in glutamate-induced  $\text{NO}$  concentration dynamics as in the coupled CBF changes. This observation may be explained either by a direct scavenging of  $\text{NO}$ , decreasing its bioavailability and thus its volume signaling, as well as by an effect along the NMDAR-nNOS pathway. Indeed, curcumin has been described to inhibit PKC activity, and subsequent phosphorylation of NR1 of the NMDA receptor, which culminates with a reduced  $\text{Ca}^{2+}$  influx and decreased nNOS catalytic activity. When the effect of curcumin was evaluated by an acute systemic administration, it was observed that it was not able to decrease the amplitude of  $\text{NO}$  and CBF signals, as it did once injected ICV, but instead it promoted a slight increase (although the time course of both dynamics were reduced). We can speculate that this difference observed depends on the route of curcumin administration, which relates with the bioavailability of curcumin, which is expectedly lower in the brain after systemic injection. Moreover, through this route, curcumin will be at least partially metabolized and thus curcumin-derivatives may also contribute to modulate both endogenous  $\text{NO}$  production and CBF, affecting the same or other signaling pathways.

Regarding epicatechin, a slight increase was observed in both  $\text{NO}$  peak concentrations and amplitude of CBF changes after ICV injection. This result agrees with a previous observation that a red wine polyphenolic powder, also containing epicatechin, administered for 4 weeks increased nNOS activity in the cerebral cortex, cerebellum and brainstem (Jendekova *et al.*, 2006). Also, epicatechin is shown to stimulate phosphorylation of the cAMP-response element binding protein, a regulator of neuronal viability and synaptic plasticity and up-regulate AMPAR GluR2 subunit (Schroeter *et al.*, 2007), which would have an impact over  $\text{NO}$  production. However, considering the time window of the observed effects, mechanisms dependent on gene expression are unlikely.

In addition to the effects over glutamate-induced  $\text{NO}$  and CBF changes, epicatechin promoted an increase in basal CBF levels. In this respect it should be mentioned that epicatechin is suggested to promote activation of the endothelial isoform of NOS in blood vessels, which is expectedly leads to vasodilation. Epicatechin-induced eNOS activation is at least partially mediated via the  $\text{Ca}^{2+}$ /CaMKII pathway (Ramirez-Sanchez *et al.*, 2010).

Based on the *in vivo* insights here presented, it is apparent that dietary polyphenols may, as a function of their structure, affect the neurovascular coupling process but, clearly, further work should be performed in order to provide robustness to the potential of both curcumin and epicatechin to modulate neuronal-derived  $\text{NO}$  and neurovascular coupling, which may include the evaluation of a chronic administration of the polyphenols.

### III. Dementia and inflammatory animal models

#### 1. Acute model of Alzheimer Disease

The glutamate-induced  $\dot{NO}$  and CBF changes were evaluated in a rat model of AD based on the intracerebroventricular injection of  $A\beta_{1-42}$  peptide. The use of direct  $A\beta$  infusion allows the study of the contribution of the amyloidogenic pathway and dissemination of the contribution of each  $A\beta$  peptide, in addition reduce significantly the experimental timeline (Lawlor and Young, 2011). In typical late-onset AD there is evidence that  $A\beta_{1-42}$  is a minor  $A\beta$  species, but it is also the earliest form and the predominant species deposited in  $A\beta_{1-42}$  the brain parenchyma (Golde *et al.*, 2000).

##### 1.1. Behaviour tests

The model of  $A\beta_{1-42}$  infusion used in this study was previously shown to be characterized by synaptotoxicity and memory impairment (Canas *et al.*, 2009) but, because the synthetic  $Ab_{1-42}$  peptide is difficult to make and given the batch-to-batch variability reported (Lawlor and Young, 2011), behavior tests were performed in  $A\beta_{1-42}$  treated rats 15 days after the injection. In brief, memory performance was evaluated by the novel object recognition and Y-maze tests. We observed that  $A\beta_{1-42}$  injection in rats brain promoted a short-term memory impairment. This conclusion is based on the observation that they spent less time exploring the novel object and in the novel arm when submitted to the novel-object recognition and Y-maze test, respectively. Relatively to the motor function there is no difference in the open field locomotion test as compared to controls (Figure 20)

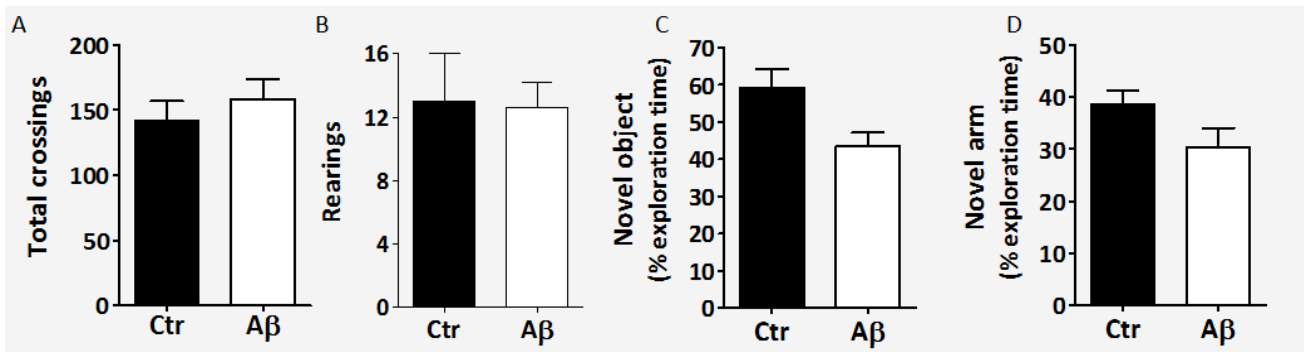


**Figure 20-** Behavior performance of Aβ<sub>1-42</sub>-treated and control rats 15 days after the injection. (A) and (B) represent the spontaneous locomotion evaluated in an open field arena regarding, respectively, the horizontal and vertical exploration. (C) Performance in novel object recognition test regarding the time spent in exploring a novel object, placed in the arena after a previous trial (2 h before) of exploration of two identical objects. (D) Performance in Y-maze regarding the time spent in exploring a novel arm, blocked in a previous exploration of the maze 2-h before. Data represents mean±SEM (n=5), (\**p* < 0.05).

### 1.2. CBF and $\dot{NO}$ Dynamics

The global results of glutamate-induced  $\dot{NO}$  and CBF changes in hippocampus of Aβ<sub>1-42</sub>-treated and control rats, 20 days after the injection, are represented in figure 21 and a detailed analysis is summarized in table 5. Regarding glutamate-induced  $\dot{NO}$  production, although no significant differences were observed in terms of  $\dot{NO}$  peak concentration between groups,  $\dot{NO}$  signals were briefer in Aβ<sub>1-42</sub>-treated rat as compared with controls (vehicle treated). Overall, in average,  $\dot{NO}$  concentration dynamic induced by glutamate was characterized by a peak concentration of  $1.36 \pm 0.06 \mu\text{M}$  and total duration of  $79 \pm 4 \text{ s}$  in control rat and a peak concentration of  $1.40 \pm 0.07 \mu\text{M}$  and total duration of  $65 \pm 5 \text{ s}$  in AD rat (*p* = 0.7111 and *p* = 0.0198 respectively, n=31 from 4 animals).

Glutamate-induced CBF changes coupled to  $\dot{NO}$  dynamics were not significantly affected by the Aβ<sub>1-42</sub> treatment, at least regarding amplitude (119.56% and 126.05% in Aβ<sub>1-42</sub>-treated and control rats, respectively, *p* = 0.5887, n=31 from 4 animals). In turn, CBF changes showed to last shorter in Aβ<sub>1-42</sub>-treated rats than in control ones (208 versus 267s, respectively, *p*=0.0474).

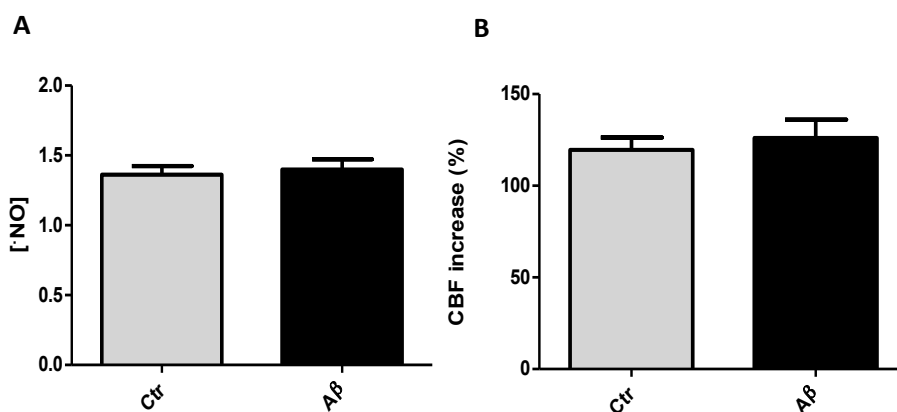


**Figure 21-** Quantitative comparison of the effect of A $\beta_{1-42}$  over glutamate-induced 'NO dynamics (A) and CBF changes (B) in rat hippocampus. Data represents mean  $\pm$  SEM. Statistical analysis was performed by Student's t-test in relation to control experiments (\* $p < 0.05$ ).

**Table 5-** Analysis of glutamate-induced 'NO signals and CBF changes in hippocampus of rats injected with A $\beta_{1-42}$  peptide and controls.

	CTR (n= 31)	A $\beta$ (n=29)	<i>P</i>	
'NO	[·NO] peak ( $\mu$ M)	1.36 $\pm$ 0.06	1.40 $\pm$ 0.07	0.7111
	Trise (s)	20 $\pm$ 3.30	19 $\pm$ 3.39	0.8901
	Ttotal (s)	80 $\pm$ 3.55	65 $\pm$ 4.92	0.0198*
	Half width (s)	44 $\pm$ 3.58	35 $\pm$ 5.15	0.1776
CBF	CBF increase (%)	120 $\pm$ 6.74	126 $\pm$ 9.95	0.5887
	Trise (s)	73 $\pm$ 4.79	64 $\pm$ 4.05	0.1642
	Ttotal (s)	267 $\pm$ 20.09	208 $\pm$ 20.96	0.0474*

### 1.3. Modulation of neurovascular coupling in AD by Curcumin

Although no statistically significant effects of curcumin were detected over 'NO-mediated neurovascular coupling under physiological conditions, we aimed to evaluate whether it had any potential to reverse differences observed in A $\beta_{1-42}$ -treated rat as compared to controls reported in the previous section. For that purpose curcumin was injected intraperitoneally (300 mg/Kg) and a representative recording is presented in Figure 22. Globally, the results were quite similar to those

obtained in naïve rats (section I), as curcumin injected IP in  $A\beta_{1-42}$ -treated rats had no strong and significant effect either at the level of  $\cdot NO$  production or CBF changes evoked by glutamate stimulus. The detailed analysis is presented in table 6. In average,  $\cdot NO$  concentration dynamics induced by glutamate in  $A\beta$  models was characterized by a peak concentration of  $3.76 \pm 0.29 \mu M$  and total duration of  $92.89 \pm 27.69$  s and a peak concentration of  $4.12 \pm 0.47 \mu M$  and total duration of  $53.75 \pm 7.74$  s, respectively, before and after curcumin, while the corresponding CBF changes were, respectively,  $159.08 \pm 11.84$  % and  $168.00 \pm 38.27$  %. However, a fine tuned observation of the recordings evidences a slight increase in the  $\cdot NO$  concentration and a decrease in the duration of  $\cdot NO$  signals after curcumin treatment that were accompanied by an increase in CBF changes.

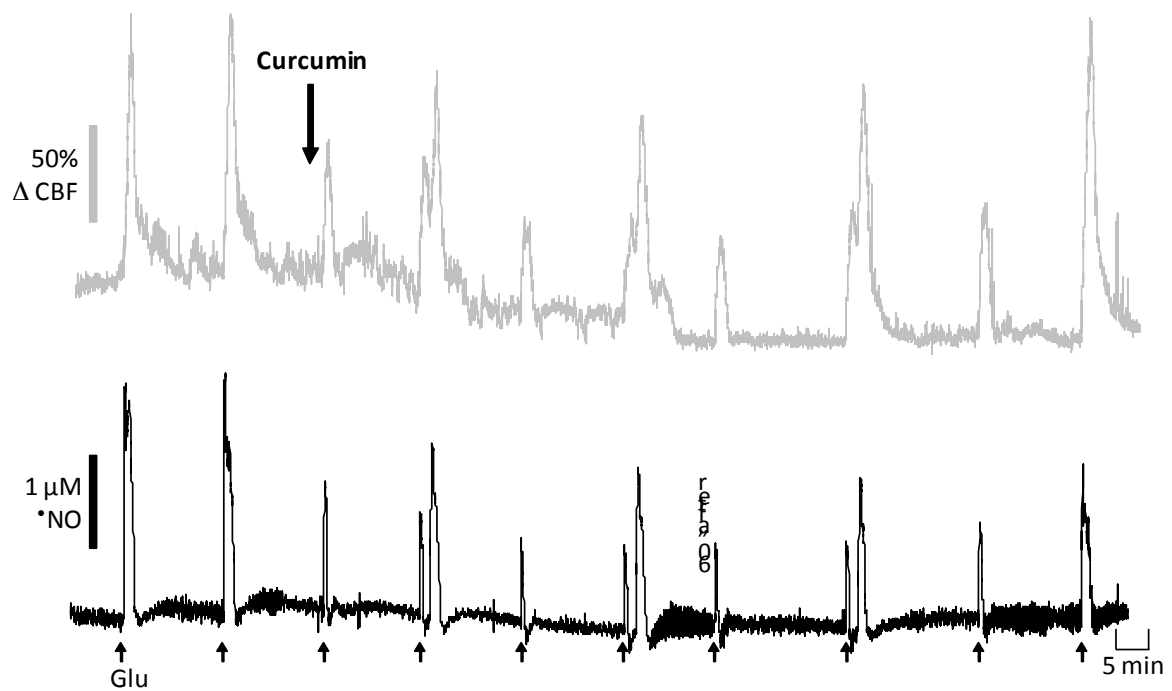


**Figure 22-** Effect of *in vivo* peripheral administration of curcumin (300 mg/kg, IP) in  $A\beta_{1-42}$ -treated rats in glutamate-induced  $\cdot NO$  dynamics (black line) and CBF changes (grey line) in rat hippocampus

**Table 6-** Analysis of glutamate-induced  $\cdot\text{NO}$  signals and CBF changes in hippocampus of  $\text{A}\beta_{1-42}$ -treated rats before and after intraperitoneal injection of curcumin

		<b>A<math>\beta</math></b> <b>(n= 19)</b>	<b>A<math>\beta</math>_Cur</b> <b>(n=4)</b>	<b>P</b>
<b><math>\cdot\text{NO}</math></b>	<b>[<math>\cdot\text{NO}</math>] peak (<math>\mu\text{M}</math>)</b>	3.76 $\pm$ 0.29	4.12 $\pm$ 0.47	0.4456
	<b>Trise (s)</b>	22 $\pm$ 4.30	11 $\pm$ 1.32	0.2074
	<b>Ttotal (s)</b>	93 $\pm$ 27.69	54 $\pm$ 7.74	0.3039
	<b>Half width (s)</b>	43 $\pm$ 5.72	34 $\pm$ 5.97	0.6161
<b>CBF</b>	<b>CBF increase (%)</b>	159 $\pm$ 11.84	168 $\pm$ 38.27	0.4191
	<b>Trise (s)</b>	57 $\pm$ 3.14	58 $\pm$ 12.40	0.7329
	<b>Ttotal (s)</b>	272 $\pm$ 22.15	220 $\pm$ 52.25	0.6299

## 2. Discussion

Neurofibrillary tangles (NFTs), insoluble  $\beta$ -amyloid ( $\text{A}\beta$ ) plaques, neuron loss,  $\cdot\text{NO}$ -related pathways and cerebrovascular dysfunction have been shown to be associated and/or contribute to the progression of AD being the major neuropathological features of this type of dementia (Hardy, 2006). However, the ascertainment of the exact role of each one of these factors still requires investigation.

The experimental approach here used, based on the direct and simultaneously measurement of  $\cdot\text{NO}$  and CBF changes in hippocampus of  $\text{A}\beta_{1-42}$ -treated rats, aimed to unravel critical mechanisms in AD, namely by providing *in vivo* critical information on how neuronal-derived  $\cdot\text{NO}$  dynamics and cerebrovascular function occur in AD. Using such approach we observed that in  $\text{A}\beta_{1-42}$ -treated rats glutamate-induced  $\cdot\text{NO}$  signals were short lasting as compared with controls, although identical regarding the peak amplitude. Previous studies developed by the host group using a triple transgenic mouse model of AD- 3xTg-AD mice also showed that  $\cdot\text{NO}$  peak concentration upon glutamatergic activation remained roughly unchanged between AD mice and controls. Only in aged 3xTg-AD mice (12 month-old) subtle differences were observed in terms of duration of the  $\cdot\text{NO}$  signals, which lasted longer as compared to nonTg mice, evidencing that the pathway of glutamate-induced  $\cdot\text{NO}$  production was not profoundly impaired. In agreement, the results here presented neither support any significant effect of  $\text{A}\beta$  over nNOS nor implicate nNOS in



the mechanisms of A $\beta$  toxicity and associated cognitive deficits, observed to occur in A $\beta_{1-42}$ -treated rats. At this respect it should be mentioned that A $\beta$  peptide has been described to both inhibit nNOS (Oliveira *et al.*, 2011) as well as stimulate nNOS activity (Stepanichev *et al.*, 2008). Indeed, Rodrigo and colleagues found that while nNOS expression was unaltered, its activity was decreased in the cerebral cortex of 16-month-old Tg2576 mice, as compared to age matched controls (Rodrigo *et al.*, 2004). On the other hand, these authors found an increase in iNOS expression and activity in cortex. Other studies have previously reported that A $\beta_{1-42}$  infusion, although promoting an impairment in working memory, fail to significantly increase in lipid peroxide levels or MDA and NOx levels (Yamada *et al.*, 1999; Cetin and Dincer, 2007).

Regarding the CBF changes coupled to  $\dot{V}$ NO dynamics we observed that in the A $\beta_{1-42}$ -treated rats neurovascular coupling was not significantly different from control animals. In turn, in 3xTg-AD mice previous work demonstrated that glutamate-induced CBF changes were significantly lower in aged 3xTg-AD mice, as compared with non-Tg, suggesting that  $\dot{V}$ NO-mediated neurovascular coupling is impaired in the later stages of AD (unpublish data). Moreover, it has been reported that many patients with Alzheimer's disease have regional cerebral hypoperfusion, which correlates to cognitive decline (Johnson *et al.*, 2005; Ruitenber, *et al.*, 2005) and that 3xTgAD mice with 11-month have a significant reduction of hippocampal vascular volume (Bourasset *et al.*, 2009). Thus, and considering that A $\beta$  is able to disrupt the physiological mechanisms regulating CBF (Niwa *et al.*, 2000b), it would be expected to obtain some degree of impairment in neurovascular coupling in A $\beta_{1-42}$ -treated rats. By promoting oxidative stress (Park *et al.*, 2004), A $\beta$  should inhibit the production of astrocytic and neuronal derived vasodilating messengers (Sun *et al.*, 2008) and thus decrease functional hyperemia. However, A $\beta$  failed to significant affect  $\dot{V}$ NO dynamics as well as that the impairment described to occur in aged 3xTgAD mice is suggested to be largely due to cerebrovascular dysfunction, rather than a dysfunctional  $\dot{V}$ NO signalling from neurons to blood vessels. The divergent observations regarding CBF changes may be explained, among other factors, by different levels of soluble A $\beta$  as well as degree and distribution of A $\beta$  deposits between both models. Accordingly, the impairment of CBF increase associated to neuronal activation seems to be more pronounced in the transgenic lines with higher A $\beta$  levels (Niwa *et al.*, 2000b). Also, different A $\beta$  fragments seems differently affect cerebrovascular function, as cerebrovascular alterations observed in transgenic mice are reproduced by superfusion of A $\beta_{1-40}$ , which predominates in vessels, but not by A $\beta_{1-42}$  (Niwa *et al.*, 2000b). Thus, our data support that A $\beta_{1-42}$  itself, although

inducing memory impairment, is unable to impair the matching of blood supply with the metabolic demands imposed by increased neuronal activity, suggesting that its deposition may be required to promote cerebrovascular dysfunction as observed in 3xTg-AD mice.

As mentioned before, in A $\beta$ <sub>1-42</sub>-treated rats glutamate-induced 'NO signals were not significantly affected regarding peak amplitudes, however, were short lasting as compared with controls, which in part may be due to increased scavenging of 'NO associated to the A $\beta$ -induced oxidative stress. Indeed, A $\beta$  seems to promote cerebrovascular effects by enhancing oxidative stress, given that the vasoactive action of A $\beta$  is counteracted by antioxidants and scavengers of RONS (Iadecola, 2003). We attempted to counteract the effects observed in A $\beta$ <sub>1-42</sub>-treated rats by acutely administering curcumin, however no significant effects were observed. Curcumin has been shown to be able to modulate a wide variety of pathways related to AD development. Indeed, curcumin has been described to have anti-amyloidogenic properties, preventing A $\beta$  aggregation through the dienone bridge present in curcumin, which is necessary to reduce plaque deposition and protein oxidation in an Alzheimer's model (Begum *et al.*, 2008). The lack of significant effects here reported however does not minimize the potential neuroprotective role of curcumin, which has been described in several studies. Curcumin extract showed to reduce glutamate-induced excitotoxicity and consequently the neurodegeneration processes in the hippocampus (Pyrzanowska *et al.*, 2010) and that both glutamate and hydroxyl radicals in the hypothalamus caused by central administration of a variety of inflammation inductors, through inhibition of the glutamate-hydroxyl radicals-PGE2 pathways. Additionally it is known that curcumin modulates levels of brain biogenic amines and 'NO in arsenic-exposed rats, where increased levels of 'NO in corpus striatum, frontal cortex as well hippocampus in arsenic-treated rats were found decreased in rats treated with curcumin (Yadav *et al.*, 2010). Also, curcumin demonstrated neuroprotective action against focal cerebral ischemic injury, as it significantly diminished infarct volume, and improved neurological deficit in a dose-dependent manner after middle cerebral artery occlusion (MCAO) (Lin, 2004, Zhao *et al.*, 2008), namely by preventing ONOO<sup>-</sup> mediated BBB damage (Jiang, 2007). Also, (Shin, 2007) suggest that curcumin is a potent inhibitor of reactive astrocyte expression and thus, prevents hippocampal cell death in mice induced by kainic acid. Thus, further experiments are required, namely by testing its effect chronically and in models of more advanced state of AD, as well by addressing its effect specifically over iNOS, the isoform responsible for the majority of 'NO-related pathological mechanisms.

### 3. Lipopolysaccharide (LPS) inflammation induction

$\text{NO}$  mediated neurovascular coupling was further addressed under inflammatory conditions. For that purpose, we used lipopolysaccharide (LPS), a component of the Gram-negative bacteria cell wall, which is a potent inducer of inflammation and has diverse effects on cells of the immune system. It was described that the intracerebral injection of LPS activated glial cells *in vivo* (Andersson, 1992; Szczepanik *et al.*, 1996) and also mimicks AD (Hausse-Wegrzyniak *et al.*, 2000; Hausse-Wegrzyniak and Wenk, 2002; Miklossy, 2008). To accomplish the objective, LPS was either injected ICV (20  $\mu\text{g}$  dissolved in 4  $\mu\text{L}$  of 0.9% NaCl) as IP (2 mg/kg), and its effects evaluated 4.5 and 24 hours later, respectively. In figure 23, it is shown a representative recording of the effects of LPS injected ICV and the effects of both ICV and IP administration routes summarized in table 8. In control conditions,  $\text{NO}$  production was characterized by a peak concentration of  $2.09 \pm 0.66 \mu\text{M}$  with a time rise of  $17 \pm 2\text{s}$  and a total duration of  $77 \pm 17$  (6 peaks analyzed from 4 individual experiments). The CBF started to increase  $7 \pm 2\text{s}$  after stimulation reaching  $103 \pm 22\%$  of the basal level after  $56 \pm 7\text{s}$  and returning to basal levels after  $368 \pm 25\text{s}$ . LPS, 4.5h after ICV injection promoted a slight decrease in duration of  $\text{NO}$  signals, although the peak concentration was unaffected. Also, regarding the coupled CBF changes, while amplitude was similar after LPS, the transient increase in CBF was short lasting. Intriguing, 24 h after LPS injected IP, while both  $\text{NO}$  peak concentrations and CBF changes remained similar to the control condition, a significant increase in the time rise was observed in  $\text{NO}$  concentration dynamics ( $p < 0.05$ ). A reasonable reason for this event could be related by the fact that pos 24h of inflammation, the levels of iNOS and ROS will be higher as we know, and thus could occur  $\text{NO}$  scavenging by specialized molecules, as we will discuss later. Also, it should be highlighted the dramatic perturbation of LPS in CBF observed after 6h, shown in Figure 23, where it appears that the increased inflammation over the time induced the crashing of neurovascular regulation and a decoupling between neuronal activity and blood supply.

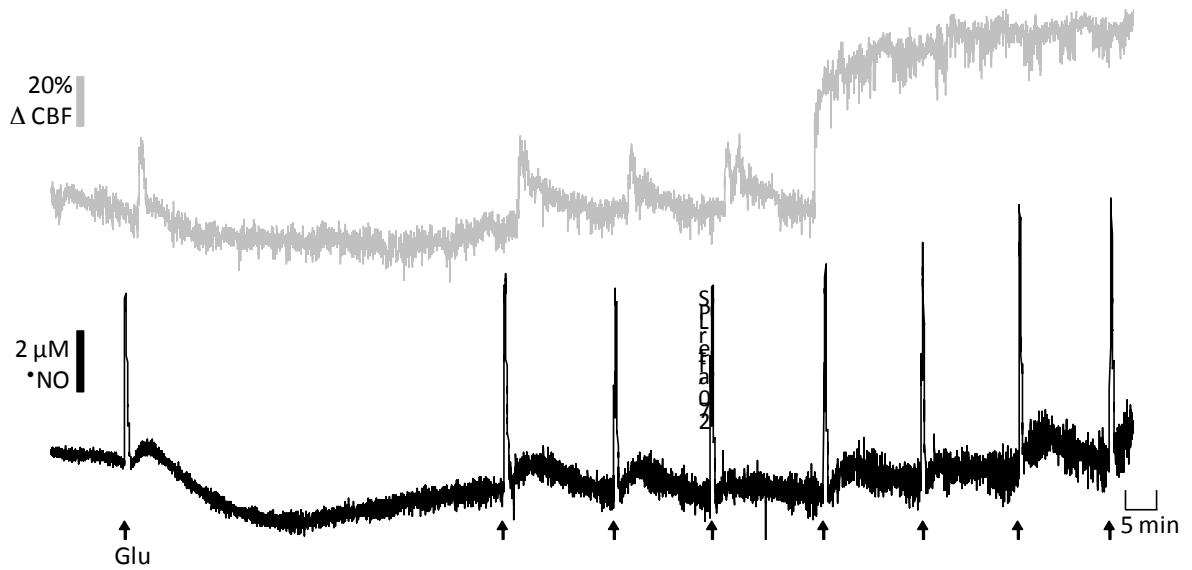


**Figure 23-** Intracerebroventricular perfusion of brain with 20  $\mu$ g of LPS followed by oxidation current records (black line), and cerebral blood changes (grey line) after Glu stimulations during approximately 6 hours of inflammation induction.

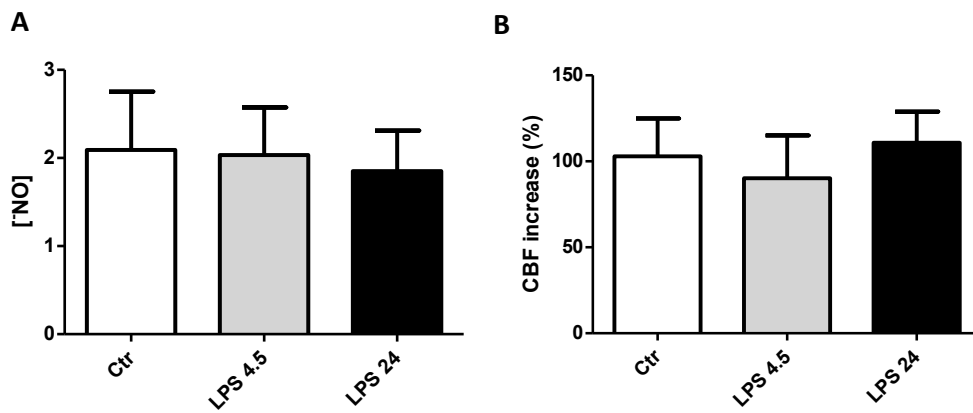


**Figure 24-** Quantitative analysis of the effect of inflammation induced by LPS injected ICV (after 4.5h) and intraperitoneally (after 24 h) over glutamate-induced  $\bullet$ NO dynamics (A) and CBF changes (B) in rat hippocampus. Data represents mean  $\pm$  SEM, ( $*p < 0.05$ ).

**Table 7-** Analysis of glutamate-induced  $\dot{\text{NO}}$  signals and CBF changes in hippocampus before and 4.5 and 24h after LPS-induced inflammation

	Ctrl (n= 6)	LPS 4.5 h (n=11)	LPS 24 h (n=4)	P (Ctrl vs 4.5)	P (Ctrl vs 24)	
$\dot{\text{NO}}$	[ $\dot{\text{NO}}$ ] peak ( $\mu\text{M}$ )	2.09 $\pm$ 0.66	2.03 $\pm$ 0.54	1.85 $\pm$ 0.46	0.9485	0.7770
	Trise (s)	17 $\pm$ 2.45	14 $\pm$ 2.90	31 $\pm$ 5.55	0.4161	0.0823
	Ttotal (s)	77 $\pm$ 17.29	59 $\pm$ 12.63	62 $\pm$ 1.31	0.4172	0.4290
	Half width (s)	31 $\pm$ 6.32	27 $\pm$ 8.10	30 $\pm$ 6.76	0.6359	0.8754
CBF	CBF increase (%)	103 $\pm$ 21.9	90 $\pm$ 24.88	111 $\pm$ 18.16	0.7091	0.7916
	Trise (s)	56 $\pm$ 6.97	47 $\pm$ 11.37	41 $\pm$ 3.66	0.4827	0.0969
	Ttotal (s)	368 $\pm$ 24.56	203 $\pm$ 34.53	286 $\pm$ 5.11	0.0029**	0.0222*

#### 4. Discussion

The bacterial inflammatory surface molecule lipopolysaccharide (LPS) is a powerful inflammatory endotoxin and amyloidogenic factor, being widely used in experimental *in vivo* models of inflammation and amyloidosis (Miklossy, 2008).

Our results of inflammatory condition, induced by ICV injection of LPS, showed that  $\dot{\text{NO}}$  concentration dynamics in hippocampus were slightly affected (reduced duration), and the same effect was observed for blood flow (Glezer *et al.*, 2003). Also, 24 h after inflammation induced systemically, duration of both  $\dot{\text{NO}}$  and CBF dynamics were reduced. In turn, the amplitude of CBF changes were less diminished after LPS injected systemically than injected within the brain. This may be associated with the antipyretic effect towards higher supply of blood cells involved in organism defense against inflammation, an elation according to Arreto and its colleagues assigning the pivotal role of macrophages for LPS which induce a dose- and time-dependent neutrophil recruitment accompanied by the generation of a tumour necrosis factor- $\alpha$  (TNF $\alpha$ )-like activity (Arreto *et al.*, 1997). It has been shown that a considerable part of NF-KB activation by LPS is linked to the NMDA/ $\dot{\text{NO}}$  pathway in CNS (Glezer *et al.*, 2003). However, the role of NF-KB as a molecule with neurodegenerative or neuroprotector actions is still enigmatic. The relevance of the intracellular cascade linking NMDA pathway to NF-KB activation is also supported by *in vitro* (Burr

and Morris, 2002) and *in vivo* studies (Madrigal *et al.*, 2001) evidencing the LPS-induced increase of nNOS/eNOS activity (Sánchez-Lemus *et al.*, 2009).

Previous studies described LPS as highly resistant to degradation by mammalian enzymes and thus constituting a persisting inflammatory stimulus. LPS activates many cell types and when administered to animals, a variety of factors are released, such as cytokines, platelet activating factor (PAF), complement-derived C5a anaphylatoxin and  $\text{NO}$  derived from iNOS. Moreover, LPS injection causes induction of expression of inducible enzyme isoforms, such as the group II extracellular phospholipase A2 (PLA2), the inducible  $\text{NO}$  synthase (iNOS) and the cyclooxygenase-2 (COX2), all contributing to the hypotensive state in septic shock (Lippolis *et al.*, 2003). Additionally (Standen *et al.*, 1989) have shown the presence of ATP-sensitive potassium ( $K_{\text{ATP}}$ ) channels on vascular smooth muscle cells, ascribing to these channels a role in the regulation of vascular tone.

Particular attention has been focused on the involvement of  $K_{\text{ATP}}$  channels in both hypotension and vascular hyporeactivity induced by endotoxemia, confirmed latter by (Lippolis *et al.*, 2003) which attribute this channels to be involved in delayed vascular hyporeactivity in rats (24h after *Escherichia coli* LPS injection). Several authors have shown the involvement of  $K_{\text{ATP}}$  channels in the early phase (within 5 h of LPS infusion) of endotoxic shock, in anaesthetized (Wu *et al.*, 1995) and unconscious rat (Gardiner *et al.*, 1999), which show the disturbance verified after 4.5 h of inflammation compared to the control.

# General Conclusions



Globally, by means of *in vivo* and measurements of  $\cdot\text{NO}$  concentration dynamics and CBF changes in  $\text{A}\beta_{1-42}$ -treated rats as well as in an inflammatory LPS rat model of dementia, this work supports a role for neuronal derived- $\cdot\text{NO}$  in cerebrovascular function in neuropathological conditions. Additionally we evaluate whether neurovascular coupling, associated with aging and neurodegeneration, may be modulated by dietary polyphenols such as curcumin and epicatechin. The potential modulation of such a process, that if impaired is related with aging and disease, would critically impact on human health.

The obtained results demonstrated that: i) acute administration of curcumin and epicatechin did not strongly and significantly affect neither  $\cdot\text{NO}$  nor CBF profiles under physiological conditions, but insights of potential modulation were provided on basis of a fine tuned observation of the recordings; ii) the neuronal-derived  $\cdot\text{NO}$  profiles were not significantly disturbed in  $\text{A}\beta_{1-42}$ -treated rats ( $\cdot\text{NO}$  signals were short lasting as compared with controls and CBF changes was not significantly different from control animals), evidencing that the pathway of glutamate-induced  $\cdot\text{NO}$  production in  $\text{A}\beta_{1-42}$ -treated rats was not profoundly impaired, although the cognitive deficits found; iii) curcumin did not show significant effects over  $\cdot\text{NO}$  dynamics and CBF changes in  $\text{A}\beta_{1-42}$ -treated rats; iv) glutamate-induced  $\cdot\text{NO}$  dynamics and coupled CBF changes were slightly reduced in LPS rat model, showing that the neurovascular coupling is compromised in inflammation rat model.



Chapter 6.

# References



- Agnati, L.F., Zoli, M., Stromberg, I. and Fuxe, K. (1995). "Intercellular communication in the brain: wiring versus volume transmission". *Neuroscience*. 69:711-26.
- Agrawal, R., Mishra, B., Tyagi, E., Nath, C., Shukla, R. (2010). "Effect of curcumin on brain insulin receptors and memory functions in STZ (ICV) induced dementia model of rat". *Pharmacol Res*. 61(3):247-52.
- Alderton, W.K., Cooper, C.E. and Knowles, R.G. (2001). "Nitric oxide synthases: structure, function and inhibition". *Biochem J*. 357:593-615.
- Andersson, P. B., Perry, V.H., and Gordon, S. (1992). "The acute inflammatory response to lipopolysaccharide in CNS parenchyma differs from that in other body tissues". *Neuroscience*, vol. 48, no. 1, pp. 169–186.
- Arreto, C.D., Dumarey, C., Nahori, M.A., Vargaftig, B.B.(1997). "The LPS-induced neutrophil recruitment into rat air pouches is mediated by TNF $\alpha$ : likely macrophage origin". *Mediators of Inflammation*. 6:335-343.
- Austin, S.A., Santhanam, A.V., Katusic, Z.S. (2010). "Endothelial nitric oxide modulates expression and processing of amyloid precursor protein". *Circ Res*. 107:1498-1502
- Barbosa, R., Lopes, A.J., Santos, R., Pereira, C., Lourenço, C.F., Ferreira, N.R., Ledo, A., Laranjinha, J. (2011). "Preparation, standardization and measurement of nitric oxide solutions". *Global Journal of Analytical Chemistry* (in press).
- Barbosa, R.M., Lourenço, C.F., Santos, R.M., Pomerleau, F., Huettl, P., Gerhardt, G.A., and Laranjinha, J. (2008). "In vivo real-time measurement of nitric oxide in anesthetized rat brain". *Methods Enzymol*. 441:351-367.
- Beckman, J.S. and Koppenol, W.H. (1996). "Nitric oxide, superoxide, and peroxynitrite: the good, the bad, and the ugly". *Am J Physiol*. 271:C1424-37.
- Bedioui, F., and Villeneuve, N. (2003). "Electrochemical nitric oxide sensors for biological samples: Principle, selected examples and applications". *Electroanalysis*. 15: 5-18.
- Begum, A.N., *et al.*, (2008). "Curcumin structure-function, bioavailability, and efficacy in models of neuroinflammation and Alzheimer's disease". *J Pharmacol Exp Ther*. 326(1):196-208.
- Bell, R.D. and Zlokovic, B.V. (2009). "Neurovascular mechanisms and blood-brain barrier disorder in Alzheimer's disease". *Acta Neuropathol*. 118:103-113.
- Blackshaw, S., Eliasson, M.J., Sawa, A., Watkins, C.C., Krug, D., Gupta, A., Arai, T., Ferrante, R.J. and Snyder, S.H. (2003). "Species, strain and developmental variations in hippocampal neuronal and endothelial nitric oxide synthase clarify discrepancies in nitric oxide-dependent synaptic plasticity". *Neuroscience*. 119:979-90.
- Bon, C.L. and Garthwaite, J. (2003). "On the role of nitric oxide in hippocampal long-term potentiation". *J Neurosci*. 23:1941-8.
- Bonner, F.T. and Sledman, G. (1996). "The chemistry of nitric oxide and redox-related species. In *Methods in Nitric Oxide Research*". Eds M. Feelisch e J. S. Stamler John Wiley & Sons Ltd. 3-18.
- Bosshart, H., Heinzelmann, M. (2007) "Targeting bacterial endotoxin: two sides of a coin". *Ann. N.Y. Acad. Sci*. 1096:1-17
- Bredl, D.S., Ferris, C.D. and Snyder, S.H. (1992). "Nitric oxide synthase regulatory sites. Phosphorylation by cyclic AMP-dependent protein Kinase, protein Kinase C, and calcium/calmodulin protein Kinase; identification of flavin and calmodulin binding sites". *J Biol Chem*. 267:10976-81.
- Bredt, D.S. and Snyder, S.H. (1990). "Isolation of nitric oxide synthetase, a calmodulin-requiring enzyme". *Proc Natl Acad Sci USA* 87(2): 682-5.
- Brown, G.C. (2001). "Regulation of mitochondrial respiration by nitric oxide inhibition of cytochrome c oxidase". *Biochim Biophys Acta* 1504(1): 46-57.
- Bruckdorfer, R. (2005). "The basics about nitric oxide". *Mol Aspects Med* 26(1-2): 3-31.
- Buee, L., Bussiere, T., Buee-Scherrer, V., Delacourte A., Hof, P.R. (2000). "Tau protein isoforms, phosphorylation and role in neurodegenerative disorders". *Brain Res Brain Res Rev*, 33:95-130.

- Burmeister, J.J., et al., (2002). "Improved ceramic-based multisite microelectrode for rapid measurements of L-glutamate in the CNS". *J. Neurosci Methods*. 119:163–171.
- Burr, P.B., Morris, B.J., (2002). "Involvement of NMDA receptors and a p21<sup>Ras</sup>-like guanosine triphosphatase in the constitutive activation of nuclear factor-kappaB in cortical neurons". *Experimental Brain Research* 147:273-279.
- Canas, P.M., Porciuncula, L.O., Cunha, G.M., Silva, C.G., Machado, N.J., Oliveira, J.M., Oliveira, C.R., Cunha, R.A. (2009). "Adenosine A2A receptor blockade prevents synaptotoxicity and memory dysfunction caused by beta-amyloid peptides via p38 mitogen-activated protein kinase pathway". *J Neurosci* 29:14741-14751.
- Cassina, A., and Radi, R. (1996). "Differential inhibitory action of nitric oxide and peroxynitrite on mitochondrial electron transport". *Arch Biochem Biophys* 328(2): 309-16.
- cellular sink". *J. Physiol. (Cambridge, U.K.)*. 536:855-862.
- Cetin, F., Dincer, S. (2007). "The effect of intrahippocampal beta amyloid (1-42) peptide injection on oxidant and antioxidant status in rat brain". *Ann N Y Acad Sci* 1100:510-517.
- Christopherson, K.S., Hillier, B.J., Lim, W.A. and Brecht, D.S. (1999). "PSD-95 assembles a ternary complex with the N-methyl-D-aspartic acid receptor and a bivalent neuronal NO synthase PDZ domain". *J Biol Chem* 274(39): 27467-73.
- Clementi, E., Brown, G.C., Feelisch, M. and Moncada S. (1998). "Persistent inhibition of cell respiration by nitric oxide: crucial role of S-nitrosylation of mitochondrial complex I and protective action of glutathione." *Proc Natl Acad Sci USA* 95(13):7631-6.
- Cooper, C.E. (1999). "Nitric oxide and iron proteins". *Biochim Biophys Acta*. 1411:290-309.
- Crane, B.R., Rosenfeld, R.J., Arvai, A.S., Ghosh, D.K., Ghosh, S., Tainer, J.A., Stuehr D.J., and Getzoff, E.D. (1999). "N-terminal domain swapping and metal ion binding in nitric oxide synthase dimerization". *Embo J* 18(22): 6271-81.
- Dall'igna, O.P., Fett, P., Gomes, M.W., Souza, D.O., Cunha, R.A., Lara, D.R. (2007). "Caffeine and adenosine A2a receptor antagonists prevent beta-amyloid (25–35)-induced cognitive deficits in rat". *Exp Neurol* 203:241–245.
- Denenberg, V.H. (1969). "Open-field Behavior in the Rat: What Does it Mean?". *Annals of the New York Academy of Sciences* 159: 852–859.
- Dev, K.K. and Morris, B.J. (1994). "Modulation of alpha-amino-3-hydroxy-5-methylisoxazole-4-propionic acid (AMPA) binding sites by nitric oxide". *J Neurochem* 63(3): 946-52.
- Drake, C.T. and Iadecola, C. (2007). "The role of neuronal signaling in controlling cerebral blood flow". *Elsevier*, 102:141-152.
- Duncan, A.J. and Heales, S.J. (2005). "Nitric oxide and neurological disorders." *Mol Aspects Med* 26(1-2): 67-96.
- Duport, S. and Garthwaite, J. (2005). "Pathological consequences of inducible nitric oxide synthase expression in hippocampal slice cultures". *Neuroscience*. 135:1155-66.
- Elfering, S.L., Sarkela, T.M., Giulivi, C. (2002). "Biochemistry of mitochondrial nitric-oxide synthase". *J Biol Chem* 277:38079-38086.
- Espey, M.G., Miranda, K.M., Thomas, D.D., Xavier, A., Cilrin, D., Vitek, M.P. and Wink D.A. (2002). "A chemical perspective on the interplay between NO, reactive oxygen species, and reactive nitrogen oxide species". *Ann. N.Y. Acad. Sci.* 962:195-206.
- Fernandez, A.P., Pozo-Rodríguez, A., Serrano, J., Martínez-Murillo, R. (2010). "Nitric oxide: target for therapeutic strategies in Alzheimer's disease". *Curr Pharm Des.* 16:2837-2850.
- Firestein, B.L. and Brecht, D.S. (1999). "Interaction of neuronal nitric-oxide synthase and phosphofructokinase". *M. J Biol Chem.* 274:10545-50.
- Fox, A. (1990). "Role of bacterial debris in inflammatory diseases of the joint and eye". *APMIS* 98 957–968.
- Frade, J., Ferreira, N., Barbosa, R., Laranjinha, J. (2005). "Mechanisms of neuroprotection of polyphenols". *Curr Med Chem* 5;307-318.
- Galleano, M., Pechanova, O., Fraga, C.G. (2010). "Hypertension, nitric oxide, oxidants, and dietary plant polyphenols". *Curr Pharm Biotechnol.* 11(8):837-48.

- Garcia, P., Youssef, I. *et al.*, (2010). "Ciliary Neurotrophic Factor Cell-Based Delivery Prevents Synaptic Impairment and Improves Memory in Mouse Models of Alzheimer's Disease". *The Journal of Neuroscience*. 30(22):7516–7527.
- Gardiner, S.M., Kemp, P.A., March, J.E. and Bennet, T. (1999). "Regional haemodynamic responses to infusion of lipopolysaccharide in conscious rats: effects of pre- or post-treatment with glybenclamide". *Br.J.Pharmacol.*, 128:1772-1778.
- Gardner, P.R., Marlin, L.A., Hall, D. and Gardner, A.M. (2001). "Dioxygen-dependent metabolism of nitric oxide in mammalian cells". *Free Redic Biol Med*. 31:191-204.
- Garthwaite, J., and Boulton, C.L. (1995). "Nitric oxide signaling in the central nervous system". *Annu. Rev. Physiol*. 57: 683–706.
- Garthwaite, J., Charles, S.L. and Chess-Williams R. (1988). "Endothelium-derived relaxing factor release on activation of NMDA receptors suggests role as intercellular messenger in the brain". *Nature* 336(6197): 385-8.
- Gendron T.F., Petrucelli L. (2009). "The role of tau in neurodegeneration". *Mol Neurodegener*, 4:13.
- Ghosh, D.K. and Stuehr, D.J. (1995). "Macrophage NO synthase: characterization of isolated oxygenase and reductase domains". reveals a head-to-head subunit interaction. *Biochemistry*. 34:801-7.
- Glezer, I., Munhoz, C.D., Kawamoto, E.M., Marcourakis, T., Avellar, M.C. and Scavone, C. (2003). "MK-801 and 7-Ni attenuate the activation of brain NF-KB induced by LPS". *Neuropharmacology* 45:1120-1129.
- Golde, T.E., Eckman, C.B., Younkin, S.G. (2000). "Biochemical detection of Abeta isoforms: implications for pathogenesis, diagnosis, and treatment of Alzheimer's disease". *Biochim Biophys Acta* 1502:172-187.
- Griffiths, C. and Garthwaite, J. (2001). "The shaping of nitric oxide signals by a
- Haley, J.E. (1998). "Gases as neurotransmitters". *Essays Biochem* 33: 79-91.
- Hamel, E. (2006). "Perivascular nerves and the regulation of cerebrovascular tone". *J Appl Physiol*. 100:1059–1064
- Hamel, E., *et al.*, (2008). "Oxidative stress and cerebrovascular dysfunction in mouse models of Alzheimer's disease". *Exp Physiol*. 93:116-120.
- Han, Y.S., Bastianetto, S., Dumont, Y., Quirion, R. (2006). "Specific plasma membrane binding sites for polyphenols, including resveratrol, in the rat brain". *J Pharmacol Exp Ther* 318: 238-245.
- Hardy, J. (2006). "A hundred years of Alzheimer's disease research" *Neuron*. 52(1):3–13.
- Hauss-Wegrzyniak B. and Wenk, G.L. (2002). "Beta-amyloid deposition in the brains of rats chronically infused with thiorphan or lipopolysaccharide: the role of ascorbic acid in the vehicle". *Neurosci Lett* 322:75-78.
- Hauss-Wegrzyniak, B., Vraniak P.D. and Wenk, G.L. (2000). "LPS-induced neuroinflammatory effects do not recover with time". *Neuroreport* 11:1759-1763.
- Hogg, N., Darley-Usmar V. M., Wilson M. T. and Moncada S. (1993). "The oxidation of alpha-tocopherol in human low-density lipoprotein by the simultaneous generation of superoxide and nitric oxide". *FEBS Lett* 326(1-3): 199-203.
- Hollmann, M. and Heinemann, S. (1994). "Cloned glutamate receptors". *Annu Rev Neurosci*. 17:31-108.
- Holscher, C. (1997). "Nitric oxide, the enigmatic neuronal messenger: its role in synaptic plasticity." *Trends Neurosci* 20(7): 298-303.
- Hossmann, K.A. (1994). "Viability thresholds and the penumbra of focal ischemia". *Annals of Neurology*, 36:557–565.
- Iadecola, C. (1998). "Cerebral circulatory dysregulation in ischemia". In M.D. Ginsberg and J. Bogousslavsky (Eds.), *Cerebrovascular diseases* (pp.319–332). Cambridge, MA: Blackwell Science.
- Iadecola, C. (2004). "Neurovascular regulation in the normal brain and in Alzheimer's disease". *Nature Reviews Neuroscience*, 5, 347–360.
- Iadecola, C. (2004). "Neurovascular regulation in the normal brain and in Alzheimer's disease". *Nat Rev Neurosci* 5:347-360.
- Iadecola, C. and Davisson, R.L. (2008). "Hypertension and Cerebrovascular Dysfunction". *Cell Metabolism Review*. 476-484.
- Jaffrey, S.R., Benfenati, F., Sbowman, A.M., Czernik, A.J. and Snyder, S.H. (2001). "Neuronal nitric-oxide synthase mediated by a ternary complex with synapsin and CAPON". *Proc Nati Avad Sci USA*. 99:3199-204.

- Jaffrey, S.R., Showman, A.M., Eliasson, M.J., Cohen, N.A. and Snyder, S.H. (1998). "CAPON: a protein associated with neuronal nitric oxide synthase that regulates its interactions with PSD95". *Neuron*. 20:115-24.
- Jendekova, L., Kojsova, S., Andriantsitohaina, R., Pechanova, O. (2006). "The time-dependent effect of provinsols<sup>TM</sup> on brain NO synthase activity in L-NAME-induced hypertension". *Physiol Res*. 55 (Suppl 1): S31-S37.
- Jeong, H.K., Jou, I. and Joe, E.H. (2010). "Systemic LPS administration induces brain inflammation but not dopaminergic neuronal death in the substantia nigra". *Journal List Mol Med*. 42(12): 823-832.
- Jiang, J., Wang, W., Sun, Y., Hu, M., Li, F. and Zhu, D. (2007). "Neuroprotective effect of curcumin on focal cerebral ischemic rats by preventing blood-brain barrier damage". *European Journal of Pharmacology*. 561:54-62.
- Johnson, N.A., *et al.*, (2005). "Pattern of cerebral hypoperfusion in Alzheimer disease and mild cognitive impairment measured with arterial spin-labeling MR imaging: initial experience". *Radiology*. 234:851-859.
- Julius, B., Enrique, S.L., Jaroslav, S. and Juan, S. (2009). "Anti-inflammatory effects of angiotensin receptor blockers in the brain and the periphery". *Cell Mol Neurobiol*. 29(6-7):781-792.
- Kanner, J., Harel, S., and Granit, R. (1991). "Nitric oxide as an antioxidant". *Arch Biochem Biophys*, 289(1): 130-6.
- Katz, D.L., Doughty, K., Ali, A. (2011) "Cocoa and chocolate in human health and disease". *Antioxid Redox Signal*.15(10):2779-811.
- Kikuchi, S., Muramatsu, H., Muramatsu, T. and Kim, S.U. (1993). "Midkine, a novel neurotrophic factor, promotes survival of mesencephalic neurons in culture". *Neurosci. Lett*. 160:9-12.
- Kim, C.H., Chung, H.J., Lee, H.K., and Haganir, R.L. (2001). "Interaction of the AMPA receptor subunit GluR2/3 with PDZ domains regulates hippocampal long-term depression". *Proc Natl Acad Sci USA* 98(20): 11725-30.
- Kojima, H., Hirotsu, M., Nakatsubo, N., Kikuchi, K., Urano, Y., Higuchi, T., Hirata Y. and Nagano T. (2001). "Bioimaging of nitric oxide with fluorescent indicators based on the rhodamine chromophore". *Anal Chem* 73(9): 1967-73.
- Koppenol, W.H. (1998). "The basic chemistry of nitrogen monoxide and peroxyxynitrite". *Free Radic Biol Med* 25(4-5): 385-91.
- Koshland, D.E., Jr. (1992). "The molecule of the year". *Science*. 258:1861.
- Kuriyama, S., Shimazu, T., Ohmori, K., Kikuchi, N., Nakaya, N., Nishino, Y., Tsubono, Y., Tsuji, I. (2006). "Green tea consumption and mortality due to cardiovascular disease, cancer, and all causes in Japan: The Ohsaki study". *JAMA*, 296:1255-1265.
- Lancaster, J. R., Jr. (1994). "Simulation of the diffusion and reaction of endogenously produced nitric oxide". *Proc Natl Acad Sci U S A* 91(17): 8137-41.
- Lancaster, J.R., Jr. (1997). "A tutorial on the diffusibility and reactivity of free nitric oxide". *Nitric Oxide*. 1:18-30.
- Law, A., Gauthier, S., Quirion, R. (2001). "Say NO to Alzheimer's disease: the putative links between nitric oxide and dementia of the Alzheimer's type". *Brain Res Brain Res Rev*. 35:73-96.
- Lawlor, P., Young, D. (2011). Chapter 17: "Ab Infusion and Related Models of Alzheimer Dementia". *NeuroMethods: Animal Models of Dementia* 48:347-370.
- Ledo, A. (2007). "Dinâmica de concentração do óxido nítrico produzido no hipocampo de rato por ativação de receptores do glutamato". UC- Coimbra: Tese de Doutorado.
- Ledo, A., Barbosa, R. M., Frade, J., and Laranjinha, J. (2002). "Nitric oxide monitoring in hippocampal brain slices using electrochemical methods". *Methods Enzymol*. 359:111-125.
- Ledo, A., Barbosa, R.M., Gerhardt, G.A, Cadenas, E., and Laranjinha, J. (2004). "Concentration dynamics of nitric oxide in rat hippocampal subregions evoked by stimulation of the NMDA glutamate receptor". *Proc Natl Acad Sci USA*. 102(48):17483-8.
- Leite, J., Junior, V., Wichert, L., Silva, R., Abud, D., Escorsi-iRosset, S., *et al.* (2009). "Neurovascular coupling and functional neuroimaging in epilepsy". *Journal of Epilepsy and Clinical Neurophysiology*. 15:1676-2649.
- Lin J.K. (2007). "Molecular targets of curcumin". *Adv Exp Med Biol*. 595:227-43.
- Lin, J.K. (2004). "Suppression of protein kinase C and nuclear oncogene expression as possible action mechanisms of cancer chemoprevention by curcumin". *Arch Pharm Res*. 27:683-692.

- Lippolis, L., *et al.*, (2003). "Dexamethasone improves vascular hyporeactivity induced by LPS in vivo by modulating ATP-sensitive potassium channels activity. *British Journal of Pharmacology*". 140, 91-96.
- Lipton, S.A. and Rosenberg, P.A. (1994). "Excitatory amino acids as a final common pathway for neurologic disorders". *N Engl J Med* 330(9): 613-22.
- Liu, P., Smith, P.F., Appleton, I., Darlington C.L. and Bilkey D.K. (2003). "Regional variations and age-related changes in nitric oxide synthase and arginase in the subregions of the hippocampus". *Neuroscience* 119(3): 679-87.
- Lo, E.H., Dalkara, T. and Moskowitz, M.A. (2003). "Mechanisms, challenges and opportunities in stroke". *Nature Reviews Neuroscience*. 4:399-415.
- Lores-Arnaiz, S., Perazzo, J.C., Prestifilippo, J.P., Lago, N., D'Amico, G., Czerniczyniec, A., Bustamante, J., Boveris, A. and Lemberg, A. (2005). "Hippocampal mitochondrial dysfunction with decreased mtNOS activity in prehepatic portal hypertensive rats". *Neurochem Int*. 47:362-8.
- Lourenço, C. (2011). "*In vivo* Nitric Oxide Concentration Dynamics Induced by Glutamatergic Neuronal Activation in Rat Brain and Its Role In Neurovascular Coupling". UC- Coimbra: Tese de Doutoramento.
- Lourenço, C., *et al.*, (2010) "In Vivo Modulation of Nitric Oxide Concentration Dynamics Upon Glutamatergic Neuronal Activation in the Hippocampus". *Hippocampus* 00:000-000.
- Lucas, K.A., Pitari, G.M., Kazerounian, S., Ruiz-Stewart, I., Park, J., Schulz, S., Chepenik, K. P. and Waldman, S. A. (2000). "Guanylyl cyclases and signaling by cyclic GMP". *Pharmacol Rev* 52(3): 375-414.
- Lynch, M. A., Errington, M.L. and Bliss, T.V. (1985). "Long-term potentiation of synaptic transmission in the dentate gyrus: increased release of [<sup>14</sup>C] glutamate without increase in receptor binding". *Neurosci Lett* 62(1): 123-9.
- Machado, A., *et al.*, (2011). "Inflammatory Animal Model for Parkinson's Disease: The Intranigral Injection of LPS Induced the Inflammatory Process along with the Selective Degeneration of Nigrostriatal Dopaminergic Neurons". *ISRN Neurology*. Article ID 476158, 16 pages.
- MacMicking, J., Xie, Q.W. and Nathan, C. (1997). "Nitric oxide and macrophage function". *Annu Rev Immunol*. 15:323-50.
- Madrigal, J.L.M., Moro, M.A., Lizasoain, I., Lorenzo, P., Castrillo, A., Bosca, L., Leza, J.C., 2001. "Inducible nitric oxide synthase expression in brain cortex after acute restrain stress is regulated by nuclear factor-B- mediated mechanism". *Journal of Neurochemistry* 76:532-538.
- Magrone, T., Jirillo, E. (2011). "Potential application of dietary polyphenols from red wine to attaining healthy ageing ". *Curr Top Med Chem*. 11(14):1780-96.
- Malinow, R. and Tsien, R.W. (1990). "Presynaptic enhancement shown by whole-cell recordings of long-term potentiation in hippocampal slices". *Nature* 346(6280): 177-80.
- Malinski, T., Taha, Z., Grunfeld, S., Patton, S., Kapturczak M. and Tomboulia P. (1993). "Diffusion of nitric oxide in the aorta wall monitored in situ by porphyrinic microsensors". *Biochem Biophys Res Commun* 193(3): 1076-82.
- Malinski, T. and Taha, Z. (1992). "Nitric oxide release from a single cell measured in situ by a porphyrinic-based microsensor". *Nature*. 358:676-8.
- Mannick, J.B. and Schonhoff, C.M. (2002). "Nitrosylation: the next phosphorylation?". *Arch Biochem Biophys* 408(1): 1-6.
- Marques, C.L. (2011). "*In vivo* Nitric Oxide Concentration Dynamics Induced by Glutamatergic Neuronal Activation in Rat Brains and its Role in Neurovascular Coupling". Tese de doutoramento em Ciências e Tecnologias da Saúde (Bioquímica), apresentada à Faculdade de Farmácia da Universidade de Coimbra.
- Martinez-Ruiz, A. and Lamas, S. (2004). "S-nitrosylation: a potential new paradigm in signal transduction." *Cardiovasc Res* 62(1): 43-52.
- McGeer, P.L. and McGeer, E.G. (2002). "Local neuroinflammation and the progression of Alzheimer's disease". *J Neurovirol* 8 529-538.

- Megson, I.L., Miller, M.R. (2009). "NO and sGC-stimulating NO donors". *Handb Exp Pharmacol*. 191:247-76.
- Mesaros, S., Grunfeld, S., Mesarosova, A., Bustin, D. and Malinski, T. (1997). "Determination of nitric oxide saturated (stock) solution by chronoamperometry on a porphyrine microelectrode". *Anal. Chim. Acta*. 339:265–270.
- Mesaros, S., Grunfeld, S., Mesarosova, A., Bustin, D., and Malinski, T. (1997). "Determination of nitric oxide saturated (stock) solution by chronoamperometry on a porphyrine microelectrode". *Anal. Chim. Acta*. 339:265–270
- Mesquita, R. (2009). "Desenvolvimento de métodos ópticos para o estudo do acoplamento neurovascular metabólico intrínseco à dinâmica cerebral". Universidade Estadual de Campinas, Instituto de Física Gleb Wataghin: Tese de Doutorado.
- Micheva, K.D., Buchanan, J., Holz, R.W. and Smith, S.J. (2003). "Retrograde regulation of synaptic vesicle endocytosis and recycling". *Nat Neurosci* 6(9): 925-32.
- Middleton, E., Kandaswami, C. and Theoharides, T.C. (2000). "The Effects of Plant Flavonoids on Mammalian Cells: Implications for Inflammation, Heart Disease, and Cancer". *Pharmacological*. 52(4): 673-751.
- Miklossy, J. (2008). "Chronic Inflammation and Amyloidogenesis in Alzheimer's Disease – Role of Spirochetes". *Journal of Alzheimer's Disease* 13:381-391.
- Miranda, K.M., Espey, M.G. and Wink, D.A. (2000). "A discussion of the chemistry of oxidative and nitrosative stress in cytotoxicity". *J Inorg Biochem*. 79:237-40.
- Münzel, T., Gori, T., Bruno, R.M., Taddei. S. (2010). "Is oxidative stress a therapeutic target in cardiovascular disease? " *Eur Heart J*. 31(22):2741-8.
- Mungrue, I.N., Bredt, D.S., Stewart, D.J., Husain M. (2003). "From molecules to mammals: what's NOS got to do with it?". *Acta Physiol Scand* 179:123-135.
- Natsume, M., Osakabe, N., Oyama, M., Sasaki, M., Baba, S., Nakamura, Y., Osawa, T., Terao, J. (2003) "Structures of (-)-epicatechin glucuronide identified from plasma and urine after oral ingestion of (-)-epicatechin: differences between human and rat". *Free Radic Biol Med*. 1;34(7):840-9.
- Niwa, K., Carlson, G.A., Iadecol, C. (2000a). "Exogenous A beta1-40 reproduces cerebrovascular alterations resulting from amyloid precursor protein overexpression in mice". *J Cereb Blood Flow Metab* 20:1659-1668.
- Niwa, K., Younkin, L., Ebeling, C., Turner, S.K., Westaway, D., Younkin, S., Ashe, K.H., Carlson, G.A., Iadecola, C. (2000b). "A beta 1-40-related reduction in functional hyperemia in mouse neocortex during somatosensory activation". *Proc Natl Acad Sci U S A* 97:9735-9740.
- Ohanian, S.H. and Schwab, J.H. (1967). "Persistence of group a streptococcal cell walls related to chronic inflammation of rabbit dermal connective tissue". *J ExpMed* 125:1137-1148.
- Oliveira, L.T., Louzada, P.R., Ferreira, S.T. (2011). "Amyloid-beta decreases nitric oxide production in cultured retinal neurons: a possible mechanism for synaptic dysfunction in Alzheimer's disease? " *Neurochem Res*. 36:163-169.
- Oyama, j., Maeda, T, Sasaki, M., Kozuma, K., Ochiai, R., Tokimitsu, I., Taguchi, S., Higuchi, Y. and Makino, N., (2010) Green Tea Catechins Improve Human Forearm Vascular Function and Have Potent Anti-Inflammatory and Anti-Apoptotic Effects in Smokers *Intern Med* 49: 2553-2559, 2010 DOI: 10.2169/internalmedicine.49.4048
- Pacher, P., Beckman, J.S. and Liaudet, L. (2007). "Nitric oxide and peroxynitrite in health and disease". *Physiol Rev* 87(1): 315-424.
- Padmaja, S. and Huie, R.E. (1993). "The reaction of nitric oxide with organic peroxy radicals". *Biochem Biophys Res Commun* 195(2): 539-44.
- Panda, K., Ghosh, S. and Stuehr, D. J. (2002). "Calmodulin activates intersubunit electron transfer in the neuronal nitric-oxide synthase dimer". *J Biol Chem* 276(26):23349-56.
- Park, L., *et al.*, (2004). "Aβ-induced vascular oxidative stress and attenuation of functional hyperemia in mouse somatosensory cortex". *J Cereb Blood Flow Metab*. 24:334–342.
- Paxinos, C. (2004). "The rat nervous system". New York: Academic Press.

- Paxinos, G., and Watson, C. (2007). "The Rat Brain in Stereotaxic Coordinates". Academic Press, New York.
- Prast, H. and Philippu, A. (2001). "Nitric oxide as modulator of neuronal function". *Prog Neurobiol.* 64:51-68.
- Puppo, A. and Halliwell, B. (1988). "Formation of hydroxyl radicals from hydrogen peroxide in the presence of iron. Is haemoglobin a biological Fenton reagent?". *Biochem J* 249(1): 185-90.
- Pyrzanowska, *et al.*, (2010). "The influence of the long-term administration of Curcuma longa extract on learning and spatial memory as well as the concentration of brain neurotransmitters and level of plasma corticosterone in aged rats". *Pharmacology, Biochemistry and Behavior* 95(3):351-358.
- Radi, R., Beckman, J.S., Bush, K.M. and Freeman, B.A. (1991). "Peroxynitrite oxidation of sulfhydryls. The cytotoxic potential of superoxide and nitric oxide". *J Biol Chem* 266(7): 4244-50.
- Ramirez-Sanchez, I., Maya, L., Ceballos, G., and Villarreal. (2010). "(-)-Epicatechin activation of endothelial cell eNOS, NO and related signaling pathways hypertension". 55(6): 1398-1405.
- Reis, F.N. (2006). "Mecanismos vasculares e plaquetares na hipertensão arterial induzida pela ciclosporina A: prevenção com um dador de NO - o 5-mononitrato de isossorbido". UC- Coimbra: Tese de Doutoramento.
- Rodrigo, J., *et al.*, (2004). "Nitric oxide in the cerebral cortex of amyloid-precursor protein (SW) Tg2576 transgenic mice". *Neuroscience* 128:73-89.
- Rombouts, S.A., *et al.*, (2005) "Delayed rather than decreased BOLD response as a marker for early Alzheimer's disease". *Neuroimage.* 26:1078-1085.
- Rossi, D.J. (2006). "Another BOLD role for astrocytes: coupling blood flow to neural activity". *Nature Neuroscience.* 9: 159-161.
- Roychowdhury, S., Noack, J., Engelmann, M., Wolf G. and Horn, T.F. (2006). "AMPA receptor-induced intracellular calcium response in the paraventricular nucleus is modulated by nitric oxide: calcium imaging in a hypothalamic organotypic cell culture model". *Nitric Oxide* 14(4): 290-9.
- Ruitenbergh, A., *et al.*, (2005). "Cerebral hypoperfusion and clinical onset of dementia: the Rotterdam study". *Ann Neurol.* 57:789-794.
- Sánchez-Lemus, E., Benicky, J., Pavel, J. and Saavedra, J.M.(2009). "In vivo Angiotensin II AT1 receptor blockade selectively inhibits LPS-induced innate immune response and ACTH release in rat pituitary gland". *Brain, Behavior, and Immunity* 23:945-957.
- Santos, R.M., Lourenço, C.F., Piedade, A.P., Andrews, R., Pomerleau, F., Huettl, P., Gerhardt, G.A., Laranjinha, J., Barbosa, R.M. (2008). "A comparative study of carbon fiber-based microelectrodes for the measurement of nitric oxide in brain tissue". *Biosens Bioelectron* 24:704-709.
- Santos, R.M., Lourenço, C.F., Pomerleau, F., Huettl, P., Gerhardt, G.A., Laranjinha, J., Barbosa, R.M. (2011). "Brain nitric oxide inactivation is governed by the vasculature". *Antioxid Redox Signal* 14:1011-1021.
- Saran, M., Michel, C. and Bors, W. (1998). "Radical functions *in vivo*: a critical review of current concepts and hypotheses". *Z Naturforsch [C].* 53:210-27.
- Schini-Kerth, V.B., Etienne-Selloum N., Chataigneau, T., Auger, C. (2011). "Vascular protection by natural product-derived polyphenols: in vitro and in vivo evidence". *Planta Med.*77(11):1161-7.
- Schlossman, J. and Hofmann, F. (2005). "cGMP-dependent protein Kinases in drug discovery". *Drug Discov Today.* 10:627-34.
- Schmitt, C.A. and Dirsch, V.M. (2009). "Modulation of endothelial nitric oxide by plant-derived products". *Nitric Oxide.* 21(2):77-91.
- Schroeter, H., Bahia, P., Spencer, J.P., Sheppard. O., Rattray, M., Cadenas, E., Rice-Evans, C., Williams, R.J. (2007). "(-)Epicatechin stimulates ERK-dependent cyclic AMP response element activity and up-regulates GluR2 in cortical neurons". *J Neurochem.* 101:1596-606.
- Schwartz, S.E. and White, W.H. (1983). "Kinetics of reactive dissolutions of nitrogen oxides into aqueous solutions. Trace atmospheric constituents. Properties, transformation and fates". New York, John Wiley and Sons: 1-117.



- Sheng, M. and Pak, D.T. (1999). "Glutamate receptor anchoring proteins and the molecular organization of excitatory synapses". *Ann N Y Acad Sci.* 868:483-93.
- Shibuki, K. and Okada, D. (1991). "Endogenous nitric oxide release required for long-term synaptic depression in the cerebellum". *Nature.* 349:326-8.
- Shibuki, K., Okada, D. (1991). "Endogenous nitric oxide release required for long-term synaptic depression in the cerebellum". *Nature.* 349:326-328.
- Shin, H.J., Lee, J.Y., et al., (2007). "Curcumin attenuates the kainic acid-induced hippocampal cell death in the mice". *Neurosci Lett.* 416(1):49-54.
- Sompamit K., Kukongviriyapan, U., Nakmareong, S., Pannangpetch, P., Kukongviriyapan, V. (2009). "Curcumin improves vascular function and alleviates oxidative stress in non-lethal lipopolysaccharide-induced endotoxaemia in mice". 616:192-199.
- Spencer, J.P., Rice-Evans, C., Williams, R.J. (2003). "Modulation of pro-survival Akt/protein kinase B and ERK1/2 signaling cascades by quercetin and its in vivo metabolites underlie their action on neuronal viability". *J. Biol. Chem.* 278:34783-34793.
- Squire, L.R., Wixted, J.T., and Clark, R.E. (2007). "Recognition memory and the medial temporal lobe: A new perspective". *Nat. Rev. Neurosci.* 8: 872–883.
- Stamler, J.S. (1994). "Redox signaling: nitrosylation and related target interactions of nitric oxide." *Cell* 78(6): 931-6.
- Standen, N.B., et al., (1989). "Hyperpolarizing vasodilators activate ATP-sensitive K<sup>+</sup> channels in arterial smooth muscle". *Science.* 245:177-180.
- Stanton, P.K., Winterer, J., Bailey, C.P., Kyrozis, A., Raginov, I., Laube, G., Veh, R.W., Nguyen, C.Q. and Muller, W. (2003). "Long-term depression of presynaptic release from the readily releasable vesicle pool induced by NMDA receptor-dependent retrograde nitric oxide". *J Neurosci* 23(13): 5936-44.
- Stefanovic, B.J., Wolfram, S., Mathias, H. and Afonso, C.S. (2007). "Functional uncoupling of hemodynamic from neuronal response by inhibition of neuronal nitric oxide synthase". *Journal of Cerebral Blood Flow & Metabolism* 27: 741–754.
- Stone, J.R. and Marletta, M.A. (1996). "Spectral and Kinetic studies on the activation of soluble guanylate cyclase by nitric oxide". *Biochemistry.* 35:1093-9.
- Stryer, L. (1995). *Biochemistry*, 4th Edition. W.H. Freeman and Company. pp. 732. ISBN 0-7167-2009-4.
- Stuehr, D., Pou, S. and Rosen, G.M. (2001). "Oxygen reduction by nitric-oxide synthases." *J Biol Chem* 276(18): 14533-6.
- Sun, H.S., Doucette, T.A., Liu, Y., Fang, Y., Teves, L., Aarts, M., Ryan, C.L., Bernard, P.B., Lau, A., Forder, J.P., Salter, M.W., Wang, Y.T., Tasker, R.A., Tymianski, M. (2008). "Effectiveness of PSD95 inhibitors in permanent and transient focal ischemia in the rat". *Stroke* 39:2544-2553.
- Sun, J., Druhan, L.J., Zweier, J.L. (2008). "Dose dependent effects of reactive oxygen and nitrogen species on the function of neuronal nitric oxide synthase. *Arch Biochem Biophys.* 471:126–133.
- Swanson. L.W., Wyss. J.M., Cowan, W.M. (1978). "An autoradiographic study of the organization of intrahippocampal association pathways in the rat". *J Comp Neurol.* 181:681-715.
- Szczepanik, A.M., Fishkin, R.J., Rush, D.K., and Wilmot, C.A., (1996). "Effects of chronic intrahippocampal infusion of lipopolysaccharide in the rat". *Neuroscience*, vol.70, no.1, pp. 57–65.
- Tatoyan, A., Giulivi, C. (1998). "Purification and characterization of a nitric-oxide synthase from rat liver mitochondria". *J Biol Chem* 273:11044-11048.
- Thomas, D.D., Liu, X., Kantrow, S.P. and Lancaster, J.R., Jr. (2001). "The biological lifetime of nitric oxide: implications for the perivascular dynamics of 'NO and O<sub>2</sub>". *Proc Natl Acad Sci U S A.* 98:355-60.
- Topel, I., Slanarius, A. and Wolf, G. (1998). "Distribution of the endothelial constitutive nitric oxide synthase in the developing rat brain: an immunohistochemical study". *Brain Res.* 788:43-8.

- Triantafilou, M., Triantafilou, K. (2005). "The dynamics of LPS recognition: complex orchestration of multiple receptors". *J.Endotoxin Res.*11:5-11.
- Vafeiadou, K., Vauzour, D., Lee, H.Y., Rodriguez-Mateos, A., Williams, R.J., Spencer, J.P. (2009). "The citrus flavanone naringenin inhibits inflammatory signalling in glial cells and protects against neuroinflammatory injury". *Arch. Biochem. Biophys.* 484:100-109.
- Van Praag, H. *et al.*, (2007). "Plant-derived flavanol (-)epicatechin enhances angiogenesis and retention of spatial memory in mice". *J Neurosci* 27:5869–5878.
- Varadarajan, S., Yatin, S., Aksenova, M., Butterfield, D.A. (2000). "Alzheimer's amyloid beta-peptide-associated free radical oxidative stress and neurotoxicity". *J Struct Biol.* 130:184-208.
- Vauzour, D., Rodriguez-Mateos, A., Corona, G., Oruna-Concha, M.J. and Spencer, J.P. (2010). "Polyphenols and Human Health: Prevention of Disease and Mechanisms of Action" *Nutrients.* 2(11):1106-1131.
- Veld, B.A., Ruitenber, A., Launer, L.J., Hofman, A., Breteler, M.M., and Stricker, B.H. (2000). "Duration of non-steroidal anti-inflammatory drug use and risk of Alzheimer's disease". The Rotterdam study, *Neurobiol Aging* 21S 204.
- Vincent, S. (2000). "Functional neuroanatomy of the nitric oxide system". Elsevier Science, BV.
- Vizi, E.S. and Kiss, J.P. (1998). "Neurochemistry and pharmacology of the major hippocampal transmitter systems: synaptic and nonsynaptic interactions". *Hippocampus.* 8:566-607.
- Vizi, E.S., Kiss, J.P. (1998). "Neurochemistry and pharmacology of the major hippocampal transmitter systems: synaptic and nonsynaptic interactions". *Hippocampus.* 8:566-607.
- Williams, R.J.; Spencer, J.P.; Rice-Evans, C. (2004). "Flavonoids: Antioxidants or signalling molecules?" *Free Radic. Biol. Med.* 36:838-849.
- Wink, D. A. and Mitchell, J. B. (1998). "Chemical biology of nitric oxide: Insights into regulatory, cytotoxic, and cytoprotective mechanisms of nitric oxide". *Free Radic Biol Med* 25(4-5): 434-56.
- Wood, J. and Garthwaite, J. (1994). "Models of the diffusional spread of nitric oxide": implications for neural nitric oxide signalling and its pharmacological properties". *Neuropharmacology.* 33:1235-44.
- Wu, C.C., Thiemermann, C. and Vane, J.R. (1995). "Glybenclamide-induced inhibition of the expression of inducible nitric oxide synthase in cultured macrophages and in the anaesthetised rat". *br. j. pharmacol.*, 114:1273-1281.
- Yadav, R.S. *et al.*, (2010). "Neuroprotective effect of curcumin in arsenic-induced neurotoxicity in rats. *Neurotoxicology.*" 31(5):533-9.
- Yamada, K., Tanaka, T., Han, D., Senzaki, K., Kameyama, T., Nabeshima, T. (1999). "Protective effects of idebenone and alpha-tocopherol on beta-amyloid-(1-42)-induced learning and memory deficits in rats: implication of oxidative stress in beta-amyloid-induced neurotoxicity *in vivo*". *Eur J Neurosci* 11:83-90.
- Youdim, K.A., Joseph, J.A. (2001). "A possible emerging role of phytochemicals in improving age-related neurological dysfunctions: A multiplicity of effects". *Free Radic. Biol. Med.*, 30:583-594.
- Youssef, I., Florent-Be ´chard, S., Malaplate-Armand, C., Koziel, V., Bihain, B., Olivier, J.L., Leininger-Muller, B., Kriem, B., Oster, T., Pillot, T. (2008). "N-truncated amyloid-beta oligomers induce learning impairment and neuronal apoptosis". *Neurobiol Aging* 29:1319–1333.
- Zhang, Y.W., Thompson, R., Zhang, H., Xu, H. (2010). "APP processing in Alzheimer's disease". *Mol Brain.* 4:3.
- Zhao, J., Zhao, Y., Zheng, W., Lu, Y., Feng, G., Yu, S. (2008). "Neuroprotective effect of curcumin on transient focal cerebral ischemia in rats". *Brain Res.* 1229:224-32.
- Zonta, M., Angulo M. C., Gobbo S., Rosengarten B., Hossmann K. A., Pozzan T. *et al.* (2003). "Neuron-to-astrocyte signaling is central to the dynamic control of brain microcirculation". *Nat Neurosci.* 6(1):43-50.